ILLINOIS

UNIVERSITY OF ILLINOIS AT URBANA-CHAMPAIGN

-

PRODUCTION NOTE

University of Illinois at
Urbana-Champaign Library
Large-scale Digitization Project, 2007.

UNIVERSITY OF ILLINOIS
BULLETIN
Vol. XXXIX November 11, 1941 No. 12

ENGINEERING EXPERIMENT STATION
BULLETIN SERIES No. 329

A STUDY OF THE COLLAPSING PRESSURE OF THIN-WALLED CYLINDERS

BY
ROLLAND G. STURM

Price: $1.50

PUBLISHED BY THE UNIVERSITY OF ILLINOIS
URBANA

[Issued weekly. Entered as second-class matter December 11, 1912, at the post office at Urbana, Illinois, under the Act of August 24, 1912. Acceptance for mailing at the special rate of postage provided for in section 1103, Act of October 3, 1917, authorized July 31, 1918]

UNIVERSITY OF ILLINOIS
ENGINEERING EXPERIMENT STATION
BULLETIN SERIES NO. 329

A STUDY OF THE COLLAPSING PRESSURE OF THIN-WALLED CYLINDERS

BY

ROLLAND GEORGE STURM
RESEARCH ENGINEER PHYSICIST ALUMINUM COMPANY OF AMERICA
(Formerly Graduate Student of University of Illinois)

PUBLISHED BY THE UNIVERSITY OF ILLINOIS

This page is intentionally blank.

CONTENTS

LIST OF FIGURES

LIST OF TABLES

A STUDY OF THE COLLAPSING PRESSURE OF THIN-WALLED CYLINDERS

I. Introduction

1. *Résumé of Previous Work.*—The problem of determining the external pressure at which a thin-walled cylinder will collapse confronts the designers of boilers, penstocks, vacuum tanks, and similar units of construction. In the design of hydro-electric or water supply projects, problems of determining the collapsing pressure of thin-walled pipe and of evaluating the effect of stiffeners upon the strength of the pipe are frequently encountered. Many industries using distillation processes under partial vacuum are confronted with the problem of designing tanks to withstand external pressure. The design of submarines involves the same problem under complicated conditions.

Many experiments have been made to determine the collapsing pressures of small pipe[1]* such as boiler tubes[2] or similar tubes[3] and of heavy-walled lap-welded steel pipe[4], but the conditions encountered in large flumes, submarines, and tanks have not been studied until recently. Such tests have been made at the A. O. Smith Corporation[5], and at the U. S. Experimental Model Basin[6]. Tests also have been made to determine the buckling strength of thin cylinders subjected to axial loads. Such tests were made for the purpose of obtaining a guide in estimating the strength of airplane fuselages[8, 9], standpipe shells[10], and to substantiate a new theory for the buckling of thin cylinders under axial compression and bending.[11]

Theoretical analyses of the behavior of cylinders under external pressures have also been made by a number of investigators. Bryan[12] obtained (in 1888) the expression for the collapsing pressure of long thin tubes by means of the energy criterion for instability. Southwell[13] obtained (in 1913) an expression for the collapse of short tubes which showed that such tubes may buckle into more than two lobes. Unfortunately, his expression contained an unknown parameter. A value for this parameter was determined (in 1914) by G. Cook[15] for the case of hinged edges and lateral pressure only. R. von Mises derived (in 1914) an equation for the collapsing strength of short thin tubes simply supported at the edges, and subjected to lateral pressure only[16], which did not contain any undetermined constants. Later (in 1929) he extended his work to include both lateral and end

*This and similar numbers refer to the bibliography at the end of the bulletin.

pressures[17]. In 1920 Sanden and Gunther[18] used von Mises' formulas in studying the behavior of stiffened thin cylinders under uniform external pressure. In 1922 Westergaard[20] presented a general conception of the buckling of elastic structures which included general equations for the gradual buckling of imperfect specimens or those with eccentric loading. In 1929 Tokugawa presented a paper[19] giving a derivation of a formula for the collapsing pressure of cylinders which includes a "frame factor" applied to the length. This frame factor is determined experimentally. The paper also included a study of the effect of stiffening rings upon the strength of the shell.

2. *Purpose and Scope of Investigation.*—The purposes of the study herein presented are

(a) to analyze the elastic behavior of thin circular cylindrical shells subjected to uniform external pressure, and to determine the pressure at which such shells collapse for simply supported and for fixed edges; extensions in the analysis are made for plastic behavior of the material, for "out-of-roundness" of the cylinder, and for stiffening effects of ring stiffeners;

(b) to study experimentally the behavior of thin-walled tubes under uniform external pressures, for comparison with the results of the theoretical analysis.

3. *Acknowledgment.*—The investigation herein reported is a part of the thesis presented by the author in partial fulfillment of the requirements for the degree of Doctor of Philosophy in Engineering at the University of Illinois in 1936.

The analytical work in the thesis and the experimental work on the steel cylinders was done under the general guidance of H. M. WESTERGAARD who at that time was Professor of Theoretical and Applied Mechanics at the University of Illinois. The experimental work on aluminum alloy cylinders was carried out in the Research Laboratories of the Aluminum Company.

The author wishes to express his gratitude to Professor H. M. WESTERGAARD for his advice and guidance; to M. L. ENGER, dean of the College of Engineering, and to F. B. SEELY, head of the Department of Theoretical and Applied Mechanics, for their encouragement and assistance; to the Aluminum Company of America for the use of its facilities; to Dr. F. C. FRARY, Director of Research and Mr. R. L. TEMPLIN, Chief Engineer of Tests of the Aluminum Company of America, for their cooperation; and to Mr. C. DUMONT, also of the Aluminum Company for his assistance with the tests.

In editing the thesis for this bulletin of the Engineering Experiment Station, W. L. SCHWALBE, Associate Professor of Theoretical and Applied Mechanics, extended the analysis of the problem to obtain the effect of certain terms that were neglected in the simplifying assumptions made in the thesis. The analysis herein presented, therefore, contains some additions to that presented in the thesis, but the final results are substantially the same. The author greatly appreciates the careful analysis given the subject by Professor SCHWALBE.

II. THEORETICAL ANALYSIS

4. *Basic Arguments and Assumptions.*—The general procedure followed in this investigation is to derive expressions for the collapsing pressures of round cylindrical shells of elastic materials, and to treat deviations from these conditions as extensions of the first derivation.

The argument used in determining the collapsing pressures is as follows: Consider the cylinder deflected into some shape such that the differential equations of continuity and equilibrium combined, together with the boundary conditions, are satisfied. If the external forces necessary to hold the shell in the deflected position are independent of the magnitude of the deflections as long as they are so small that they do not materially change the general shape of the shell, then the shell is in a state of neutral equilibrium. The lowest pressure at which neutral equilibrium may begin is the critical or collapsing pressure of the cylinder. Below the critical pressure the equilibrium is stable, above the critical value the equilibrium is unstable.

The assumptions involved in setting up the general differential equations are as follows:

(1) The shell is a round cylinder before buckling.

(2) The shell is of uniform thickness throughout.

(3) The material in the shell is homogeneous and isotropic, and is elastic according to Hooke's law.

(4) The thickness of the shell wall is small compared to the diameter, so that the distribution of normal stress over the thickness may be assumed as linear.

(5) As a consequence of the preceding assumption, the radial stress, σ_z, is negligible compared to the circumferential and longitudinal stresses, and the radial shearing detrusions are zero.

(6) Displacements are small compared to the thickness so that

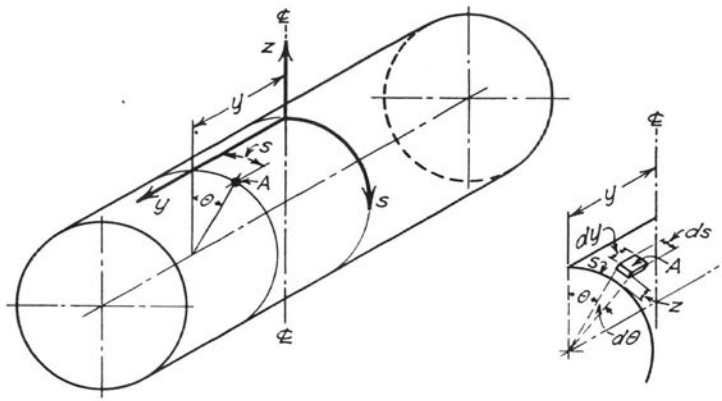

FIG. 1. SYSTEM OF COORDINATES

certain small quantities may be neglected. Neglections are indicated in the development of the analysis.

5. *System of Coordinates.*—The system of cylindrical coordinates used to define and locate any particular element of shell is indicated in Fig. 1. The whole system is based on a reference cylinder the radius of which is the average mean radius of the actual shell, and the longitudinal axis of which coincides with that of the actual shell. The origin of coordinates is taken on the cylinder of reference, at the point of maximum radial displacement of the deflected shell, and midway between the ends of the cylinder.

The y-axis is parallel to the axis of the shell, and lies on the cylinder of reference, positive toward the reader.

The s-axis lies on the circumference of a right section of the cylinder of reference, positive in a clockwise direction. The coordinate is $s = R\theta$ where R is the radius of the cylinder of reference, and θ is the angle subtended by s in a right section of the cylinder of reference.

The z-axis coincides with the radius of the cylinder of reference, the radial displacement z being measured positive outward.

The meanings of all symbols used in the subsequent pages are given in the following section.

6. *Notation.*—In the discussion the following notation is used:

A = constant (indeterminate in magnitude at collapse), represents the maximum value of deflection

A_o = maximum initial departure from a round cylinder

a, b, c = arbitrary numerical constants determined from boundary conditions and the general differential equation

B, C = constants determined by the differential equations

D = diameter of cylinder, inches

E = modulus of elasticity of the material in the shell or in the stiffener, lb. per sq. in.

E' = effective modulus of elasticity, lb. per sq. in.

E_1 = tangent modulus for the average stress, S_1, in the plastic range, lb. per sq. in.

EI_s = flexural rigidity of combined stiffener and shell in length, L_s, lb.-in.^{2}

$I = \frac{t^3}{12}$ = moment of inertia per unit of length of shell, in.^{3}

I_s = moment of inertia of combined stiffener and plate, in.^{4}

K = numerical coefficient dependent upon the ratios of L/D and D/t such that $W_c = KE\left(\frac{t}{D}\right)^3$

$K_1, K_2, K', K'', K_1', K_2', K_1'', K_2''$ = numerical coefficients, dependent upon the ratios of L/D and D/t used in evaluating K

L = length of cylinder, inches

L_o = length of one wave under end load only, inches

L_s = stiffener spacing, inches

M_{st} = bending moment in the stiffener, in.-lb.

N = number of lobes into which the shell collapses

P = end load in addition to external pressure, lb. per linear inch

P_c = end load causing collapse, end load only, lb. per linear inch

Q = the elastic limit of the material in the shell, lb. per sq. in.; this value may be taken as 1.1 times the proportional limit as determined by Tuckerman[32]

R_s = radius from center of cylinder to the centroid of a right section of the stiffener and the plate effective with it, inches

r, r' = numerical ratios dependent on R/L and N introduced by loading conditions

S = maximum total stress in the shell (direct stress and bending), lb. per sq. in.

$\overline{S}$ = allowable total stress in an out-of-round shell, lb. per sq. in.

S_1 = average stress in the shell, lb. per sq. in.

$S_c = P_c/t$ = unit longitudinal stress corresponding to P_c, lb. per sq. in.

S_p = unit longitudinal stress corresponding to an axial load whether tension or compression, lb. per sq. in.

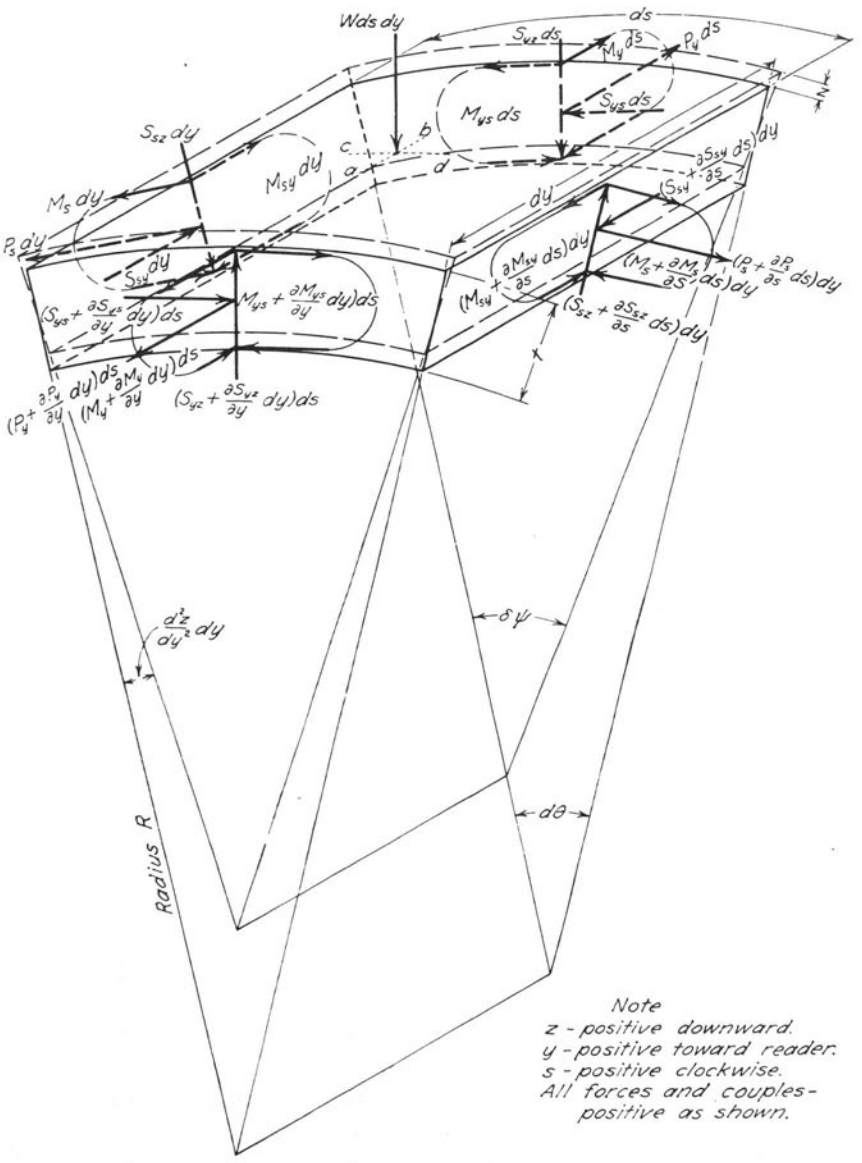

FIG. 2. ELEMENT OF SHELL IN EQUILIBRIUM

S_u = modulus of failure of the material in the shell; the tensile strength of the material may be used for S_u, lb. per sq. in.
S_y = yield strength of the material, lb. per sq. in.
S_z = maximum circumferential bending stress in the deflected shell, lb. per sq. in.
t_s = thickness of unstiffened shell having the same strength as the stiffened shell, inches
W = the actual pressure applied, lb. per sq. in.
$\overline{W}$ = allowable pressure of an out-of-round shell, lb. per sq. in.
W_c = the collapsing pressure for the shell, lb. per sq. in.
W_s = external pressure at collapse of the stiffened shell, lb. per sq. in.
W_u = ultimate collapsing pressure of an actual imperfect tube, lb. per sq. in.
Z_s = radial deflection of the stiffener, inches
Z_o = initial departure from a round cylinder, inches
$\alpha = \left(\frac{N^2L^2}{\pi^2R^2} + 1\right)$ = numerical ratio dependent on R/L and N
βE = slope of the tangent to the stress–strain curve at the yield strength, lb. per sq. in. (β = 0.10 to 0.20 for materials not cold worked, and β = 0.05 to 0.10 for materials cold worked appreciably)
γ_{sy} = unit-detrusion in a tangential plane
ϵ_s = unit-strain in the circumferential direction
ϵ_y = unit-strain in the longitudinal direction
$\lambda = \left(\frac{\pi^2R^2}{N^2L^2} + 1\right)$ = numerical ratio dependent on R/L and N
μ = Poisson's ratio
ϵ_z = unit-strain in radial direction
z = radial deflection of middle surface
u = longitudinal displacement of a point in the middle surface
v = circumferential displacement of a point in the middle surface.

7. *Deformed Element of Shell.*—The element of shell considered is shown in its deformed state* in Fig. 2. If u, v, and z are the displacements in the directions y, s, and z, respectively, of a point in the middle surface of the shell from the undeformed position, then the strains and the detrusion of the middle surface are defined as

$$\epsilon_y = \frac{\partial u}{\partial y}, \qquad \epsilon_s = \frac{\partial v}{\partial s} + \frac{v}{R}, \qquad \gamma_{sy} = \frac{\partial u}{\partial s} + \frac{\partial v}{\partial y}. \tag{1}$$

*A more complete description of a deformed element is given in Reference 34, p. 77.

By eliminating u and v, the following equation of compatibility[21, 22] is obtained:

$$\frac{\partial^2 \epsilon_s}{\partial y^2} + \frac{\partial^2 \epsilon_y}{\partial s^2} - \frac{\partial^2 \gamma_{sy}}{\partial s \partial y} - \frac{1}{R}\frac{\partial^2 z}{\partial y^2} = 0. \tag{2}$$

$\delta\psi$ is the infinitesimal angle at the center of curvature of the deflected shell, subtended by the circumferential element of length. It may be expressed as a function of θ; $\delta\psi = \frac{\partial \psi}{\partial \theta} d\theta$, and consists of the following parts:

(1) $d\theta$, original angle

(2) $-\frac{1}{R}\frac{\partial^2 z}{\partial \theta^2} d\theta$, due to change in slope over length ds

(3) $-\frac{z}{R} d\theta$, due to radial deflection

(4) $\epsilon_s d\theta$, due to circumferential strain.

Hence

$$\frac{\partial \psi}{\partial \theta} = 1 - \frac{1}{R}\frac{\partial^2 z}{\partial \theta^2} - \frac{z}{R} + \epsilon_s. \tag{3}$$

8. *Internal Forces and Couples.*—In Fig. 2 are shown the forces and couples holding the element of shell in equilibrium.

External Force:

W = external pressure, lb. per sq. in.

Normal Forces:

(Positive when acting in the positive direction on the face of an element facing the positive direction)

P_s = normal force acting on a unit of length of the face of the element lying in a plane normal to the circumferential tangent to the shell, lb. per linear in.

P_y = normal force acting on a unit of length of the face of the element lying in a plane normal to the longitudinal tangent to the shell, lb. per linear in.

Shearing Forces:

(Positive when acting in the positive direction on the face of an element facing the positive direction)

S_{sy} = shearing force in the y direction on the unit of length of the face of the element lying in a plane normal to the circumferential tangent to the shell, lb. per linear in.

S_{ys} = shearing force in the s direction on a unit of length of the face of the element lying in a plane normal to the longitudinal tangent to the shell, lb. per linear in.

S_{sz} = shearing force in the z direction on a unit of length of the face of the element lying in a plane normal to the circumferential tangent to the shell, lb. per linear in.

S_{yz} = shearing force in the z direction on a unit of length of the face of the element lying in a plane normal to the longitudinal tangent to the shell, lb. per linear in.

Couples:

(Positive where the force of the couple farther away from the center of the shell is positive)

M_s = bending couple or moment resulting from the distribution of normal forces on a unit of length of the face of the element lying in a plane normal to the circumferential tangent to the shell, in.-lb. per in.

M_y = bending couple or moment resulting from the distribution of normal forces on a unit of length of the face of the element lying in a plane normal to the longitudinal tangent to the shell, in.-lb. per in.

M_{sy} = twisting couple or moment resulting from the distribution of shearing forces on a unit of length of face of the element lying in a plane normal to the circumferential tangent to the shell, in.-lb. per in.

M_{ys} = twisting couple or moment resulting from the distribution of shearing forces on a unit of length of the face of the element lying in a plane normal to the longitudinal tangent to the shell, in.-lb. per in.

9. *Internal Forces and Couples in Terms of Displacement.*—On the basis of Hooke's law the normal and shearing forces may be expressed in terms of the strains and detrusion as follows:[21, 22, 34]

$$P_y = \frac{Et}{1 - \mu^2} (\epsilon_y + \mu\epsilon_s) \tag{4}$$

$$P_s = \frac{Et}{1 - \mu^2} (\epsilon_s + \mu\epsilon_y) \tag{5}$$

$$S_{sy} = \frac{Et}{2 (1 + \mu)} \gamma_{sy}. \tag{6}$$

The moments in terms of displacement, z, are:

$$M_y = -\frac{EI}{1 - \mu^2} \left(\frac{\partial^2 z}{\partial y^2} + \frac{\mu}{R^2} \frac{\partial^2 z}{\partial \theta^2} + \mu \frac{z}{R^2} \right) \tag{7}$$

$$M_s = -\frac{EI}{1 - \mu^2} \left(\frac{1}{R^2} \frac{\partial^2 z}{\partial \theta^2} + \frac{z}{R^2} + \mu \frac{\partial^2 z}{\partial y^2} \right) \tag{8}$$

$$M_{sy} = -\frac{EI}{1 - \mu^2} (1 - \mu) \frac{1}{R} \frac{\partial^2 z}{\partial \theta \partial y}. \tag{9}$$

In the derivation of Equation (9) it is assumed that the difference between M_{sy} and M_{ys} is negligibly small. If this assumption is not made, the left side of Equation (9) becomes $\frac{1}{2} (M_{sy} + M_{ys})$.

The values for ϵ_s, ϵ_y, γ_{sy} from Equations (4), (5), and (6) are substituted into Equation (2). The result is

$$\frac{\partial^2 P_s}{\partial y^2} - \mu \frac{\partial^2 P_y}{\partial y^2} + \frac{1}{R^2} \frac{\partial^2 P_y}{\partial \theta^2} - \frac{\mu}{R^2} \frac{\partial^2 P_s}{\partial \theta^2} - \frac{2 (1 + \mu)}{R} \frac{\partial^2 S_{sy}}{\partial \theta \partial y} = \frac{Et}{R} \frac{\partial^2 z}{\partial y^2}. \tag{10}$$

10. *Equations of Equilibrium.*—The conditions of equilibrium applied to the force system shown in Fig. 2, neglecting differentials of higher order than the second, give the following equations:

$$\frac{\partial P_s}{\partial s} + \frac{\partial S_{ys}}{\partial y} + S_{sz} \frac{\partial \psi}{\partial s} = 0 \tag{11}$$

$$\frac{\partial P_y}{\partial y} + \frac{\partial S_{sy}}{\partial s} - S_{yz} \frac{\partial^2 z}{\partial y^2} = 0 \tag{12}$$

$$\frac{\partial S_{sz}}{\partial s}+\frac{\partial S_{yz}}{\partial y}=W+P_s\frac{\partial \psi}{\partial s}-P_y\frac{\partial^2 z}{\partial y^2}-S_{ys}\frac{\partial^2 z}{\partial s\partial y}-S_{sy}\frac{\partial^2 z}{\partial y\partial s} \tag{13}$$

$$S_{yz}=\frac{\partial M_y}{\partial y}+\frac{\partial M_{sy}}{\partial s} \tag{14}$$

$$S_{sz}=\frac{\partial M_s}{\partial s}+\frac{\partial M_{ys}}{\partial y} \tag{15}$$

$$S_{sy}-S_{ys}+M_{sy}\frac{\partial \psi}{\partial s}+M_{ys}\frac{\partial^2 z}{\partial y^2}=0. \tag{16}$$

If products of forces and moments with the derivatives of displacements, which are small by comparison with unity, are neglected, and the shearing forces are eliminated from Equations (11) and (12) by means of Equations (14), (15), and (16), then, with $M_{sy}=M_{ys}$, the following equation is obtained:

$$\frac{\partial^2 P_s}{\partial s^2}-\frac{\partial^2 P_y}{\partial y^2}+\frac{1+\epsilon_s}{R}\frac{\partial^2 M_s}{\partial s^2}+\frac{2(1+\epsilon_s)}{R}\frac{\partial^2 M_{sy}}{\partial s\partial y}=0. \tag{17}$$

Equations (14) and (15) are combined with Equation (13); then

$$\frac{\partial^2 M_y}{\partial y^2}+2\frac{\partial^2 M_{sy}}{\partial s\partial y}+\frac{\partial^2 M_s}{\partial s^2}=W+P_s\frac{\partial \psi}{\partial s}-P_y\frac{\partial^2 z}{\partial y^2}-S_{ys}\frac{\partial^2 z}{\partial s\partial y}-S_{sy}\frac{\partial^2 z}{\partial s\partial y}. \tag{18}$$

11. *General Differential Equations.*—The moments from Equations (7), (8), and (9) are substituted into Equation (18); then

$$-\frac{EI}{1-\mu^2}\left(\frac{\partial^4 z}{\partial y^4}+\frac{\mu}{R^2}\frac{\partial^2 z}{\partial y^2}+\frac{2}{R^2}\frac{\partial^4 z}{\partial\theta^2\partial y^2}+\frac{1}{R^4}\frac{\partial^4 z}{\partial\theta^4}+\frac{1}{R^4}\frac{\partial^2 z}{\partial\theta^2}\right)=W+P_s\frac{1}{R}\frac{\partial \psi}{\partial\theta}-P_y\frac{\partial^2 z}{\partial y^2}-S_{ys}\frac{1}{R}\frac{\partial^2 z}{\partial\theta\partial y}-S_{sy}\frac{1}{R}\frac{\partial^2 z}{\partial\theta\partial y}. \tag{19}$$

A second equation is obtained from Equations (17), (8), and (9):

$$\frac{1}{R^2}\frac{\partial^2 P_s}{\partial\theta^2} - \frac{\partial^2 P_y}{\partial y^2} - \frac{(1+\epsilon_s)}{R}\frac{EI}{(1-\mu^2)}\left(\frac{1}{R^4}\frac{\partial^4 z}{\partial\theta^4} + \frac{1}{R^4}\frac{\partial^2 z}{\partial\theta^2} + \frac{(2-\mu)}{R^2}\frac{\partial^4 z}{\partial\theta^2\partial y^2}\right) = 0. \qquad (20)$$

A third equation is obtained from the equation of compatibility (10), combined with Equation (12), in which the small quantity $S_{ys}\dfrac{\partial^2 z}{\partial y^2}$ is neglected:

$$\frac{\partial^2 P_s}{\partial y^2} + (2+\mu)\frac{\partial^2 P_y}{\partial y^2} + \frac{1}{R^2}\frac{\partial^2 P_y}{\partial\theta^2} - \frac{\mu}{R^2}\frac{\partial^2 P_s}{\partial\theta^2} = \frac{Et}{R}\frac{\partial^2 z}{\partial y^2}. \qquad (21)$$

A fourth equation is obtained by differentiating the strain

$$\epsilon_s = \frac{1}{Et}(P_s - \mu P_y) = \frac{1}{R}\left(\frac{\partial v}{\partial\theta} + z\right)$$

twice with respect to y, giving

$$\frac{\partial^2 P_s}{\partial y^2} - \mu\frac{\partial^2 P_y}{\partial y^2} = \frac{Et}{R}\left(\frac{\partial^3 v}{\partial y^2\partial\theta} + \frac{\partial^2 z}{\partial y^2}\right). \qquad (22)$$

The simultaneous Equations (19), (20), (21), and (22) represent the relations between the radial and circumferential deflections z and v, and the forces P_s, P_y, S_{ys}, S_{sy}, and W, for a thin cylindrical shell which is not stressed beyond the elastic limit and which has small deflections.

To determine the external pressure W, the end load P_y, the shearing stress S_{sy} (or S_{ys}), or any combination of these forces at which the equilibrium of the shell becomes indifferent, the shell is considered in the deflected shape which satisfies the foregoing differential equations and the boundary conditions. The function, z, representing this deflection must meet the requirement that its magnitude is indeterminate for some value of the external force. This value of the external force at which the condition of neutral equilibrium prevails is the critical load on the cylinder.

III. Solution of Buckling Equations for Round Cylinders, Without Stiffeners

12. *Uniform Pressure Applied to Sides Only.*—For this type of loading the value of the circumferential force per unit length of shell, P_s, may be expressed as

$$P_s = -WR + f(y, s).$$

WR is the average value of P_s and f is a function of y and s which expresses the variation of P_s from the average value. When the deflection, z, of the shell is very small, then $f(y, s)$ is also very small.

The longitudinal force, P_y, has an average value of zero, for this loading and the value of P_y at any point departs from this average by a small amount $g(y, s)$, dependent upon the deflection z. This gives

$$P_y = 0 + g(y, s).$$

The shearing forces S_{sy} and S_{ys} have average values of zero for this case of loading with variations from the average value by amounts $h(y, s)$ and $j(y, s)$, respectively:

$$S_{ys} = 0 + h(y, s) \qquad S_{ys} = 0 + j(y, s).$$

The values of P_s, P_y, S_{sy}, and S_{ys} are substituted into Equations (19), (20), (21), and (22), and products such as f with terms in $\frac{\partial\psi}{\partial\theta}$ other than unity, $g\frac{\partial^2 z}{\partial s\partial y}$, $h\frac{\partial^2 z}{\partial s\partial y}$, and $j\frac{\partial^2 z}{\partial s\partial y}$ are neglected.

Then

$$\frac{EI}{1-\mu^2}\left[\frac{\partial^4 z}{\partial y^4} + \frac{\mu}{R^2}\frac{\partial^2 z}{\partial y^2} + \frac{2}{R^2}\frac{\partial^4 z}{\partial\theta^2\partial y^2} + \frac{1}{R^4}\left(\frac{\partial^2 z}{\partial\theta^2} + \frac{\partial^4 z}{\partial\theta^4}\right)\right] + \frac{1}{R}f(y, s) = -W\left(\frac{1}{R}\frac{\partial^2 z}{\partial\theta^2} + \frac{z}{R} - \epsilon_s\right) \tag{23}$$

$$\frac{1}{R^2}\frac{\partial^2 f}{\partial\theta^2} - \frac{\partial^2 g}{\partial y^2} - \frac{(1+\epsilon_s)}{R^3}\frac{EI}{(1-\mu^2)}\left(\frac{1}{R^2}\frac{\partial^4 z}{\partial\theta^4} + \frac{1}{R^2}\frac{\partial^2 z}{\partial\theta^2} + (2-\mu)\frac{\partial^4 z}{\partial\theta^2\partial y^2}\right) = 0 \tag{24}$$

$$(2+\mu)\frac{\partial^2 g}{\partial y^2}+\frac{1}{R^2}\frac{\partial^2 g}{\partial \theta^2}+\frac{\partial^2 f}{\partial y^2}-\frac{\mu}{R^2}\frac{\partial^2 f}{\partial \theta^2}=\frac{Et}{R}\frac{\partial^2 z}{\partial y^2} \tag{25}$$

$$\frac{\partial^2 f}{\partial y^2}-\mu\frac{\partial^2 g}{\partial y^2}=\frac{Et}{R}\left(\frac{\partial^3 v}{\partial y^2 \partial \theta}+\frac{\partial^2 z}{\partial y^2}\right). \tag{26}$$

(a) *Edges of Shell at Ends Simply Supported.*—The boundary conditions for z are $z = 0$, $\frac{\partial^2 z}{\partial y^2} = \frac{\partial^2 z}{\partial \theta^2} = 0$ for all values of θ when $y = \pm\frac{L}{2}$. Because of symmetry $\frac{\partial z}{\partial \theta} = 0$ for all values of θ when $y = 0$, and $\frac{\partial z}{\partial \theta} = 0$ for all values of y at $\theta = 0$.

For the circumferential displacement, $\frac{\partial v}{\partial \theta} = 0$ for all values of θ at $y = \pm\frac{L}{2}$.

These conditions suggest solutions of the form,

$$z = A\cos N\theta\cos\frac{\pi y}{L}$$
$$v = B\sin N\theta\cos\frac{\pi y}{L}. \tag{27}$$

Figure 3 shows cross-sections of a shell deflected in various ways so that $N = 2$, 3, and 4, giving respectively two, three, and four lobes. The number of lobes has been found to depend upon the proportions of the shell and for any given shell will be that number which will give the lowest pressure at neutral equilibrium.

When z and v are substituted into Equations (23), (24), (25), and (26) the following equations result:

$$\frac{EI}{1-\mu^2}\left[\frac{\pi^4}{L^4}+\frac{(2N^2-\mu)\pi^2}{R^2L^2}-\frac{N^2}{R^4}+\frac{N^4}{R^4}\right]A\cos N\theta\cos\frac{\pi y}{L}$$
$$=\frac{W}{R}(AN^2+BN)\cos N\theta\cos\frac{\pi y}{L}-\frac{1}{R}f(y,s) \tag{28}$$

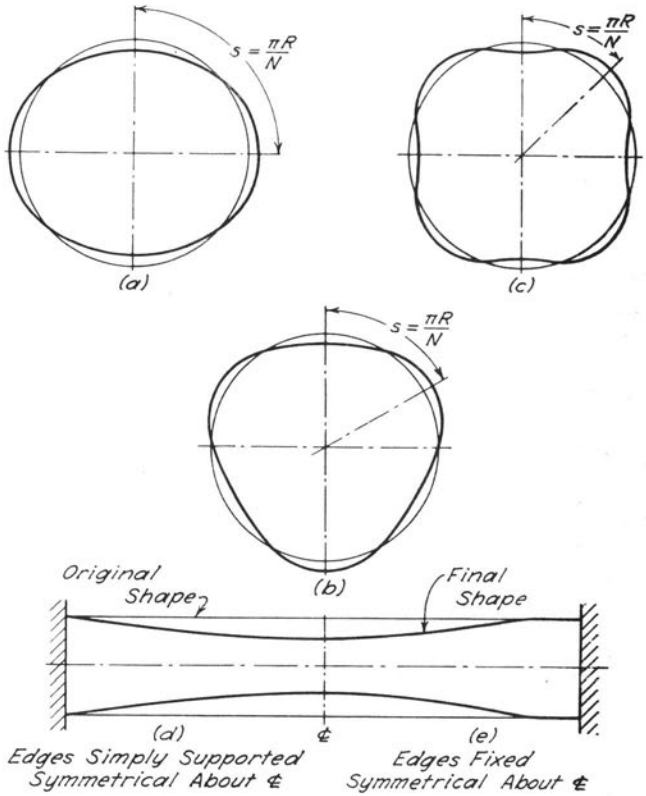

FIG. 3. SECTIONS OF DEFLECTED CYLINDERS

$$\frac{1}{R^2}\frac{\partial^2 f}{\partial\theta^2} - \frac{\partial^2 g}{\partial y^2} = \frac{(1-\epsilon_s)}{R^3}\frac{EI}{(1-\mu^2)}\left[\frac{N^4}{R^2} - \frac{N^2}{R^2} + (2-\mu)\frac{N^2\pi^2}{L^2}\right] A\cos N\theta\cos\frac{\pi y}{L} \tag{29}$$

$$(2+\mu)\frac{\partial^2 g}{\partial y^2} + \frac{1}{R^2}\frac{\partial^2 g}{\partial\theta^2} + \frac{\partial^2 f}{\partial y^2} - \frac{\mu}{R^2}\frac{\partial^2 f}{\partial\theta^2} = -\frac{Et}{R}\frac{\pi^2}{L^2} A\cos N\theta\cos\frac{\pi y}{L} \tag{30}$$

$$\frac{\partial^2 f}{\partial y^2} - \mu\frac{\partial^2 g}{\partial y^2} = -\frac{Et}{R}\frac{\pi^2}{L^2}(BN + A)\cos N\theta\cos\frac{\pi y}{L}. \tag{31}$$

From Equation (28) it follows that $f(y, s)$ has the form

$$f(y, s) = C \cos N\theta \cos \frac{\pi y}{L}$$

and from Equations (29) and (30) that $g(y, s)$ has a similar form,

$$g(y, s) = D \cos N\theta \cos \frac{\pi y}{L}.$$

From Equation (31)

$$BN + A = \frac{R}{Et}(C - \mu D).$$

The values of C and D are found to be

$$\frac{C}{A} = \frac{Et}{R\alpha^2} - \frac{Et}{R^3(1-\mu^2)}\left[N^2\{1+(\lambda-1)(2-\mu)\}-1\right]\left(1-\frac{WR}{Et}\right)\frac{\alpha+1+\mu}{\lambda\alpha}$$

$$\frac{D}{A} = \frac{Et}{R\lambda\alpha} + \frac{Et}{R^3(1-\mu^2)}\left[N^2\{1+(\lambda-1)(2-\mu)\}-1\right]\left(1-\frac{WR}{Et}\right)\frac{1-\mu(\alpha-1)}{\lambda\alpha}$$

in which

$$\lambda = \frac{\pi^2 R^2}{N^2 L^2} + 1$$

and

$$\alpha = \frac{N^2 L^2}{\pi^2 R^2} + 1.$$

From Equation (28)

$$\left[\frac{Et}{R^2\alpha^2}-\frac{EI}{R^4(1-\mu^2)}\frac{(\alpha+1+\mu)}{\lambda\alpha}\left[N^2\{1+(\lambda-1)\,(2-\mu)\}-1\right]\right]\mathrm{A}\cos N\theta\cos\frac{\pi y}{L}$$

$$+\frac{EI}{R^4(1-\mu^2)}N^2[N^2\lambda^2-\mu(\lambda-1)-1]\,A\cos N\theta\cos\frac{\pi y}{L}=\frac{W}{R}FA\cos N\theta\cos\frac{\pi y}{L}\quad(32)$$

where

$$F=N^2-1+\frac{1}{\alpha^2}-\frac{\mu}{\lambda\alpha}$$

$$-\frac{I}{R^2(1-\mu^2)t\lambda\alpha}[N^2\{1+(\lambda-1)(2-\mu)\}-1]\left\{\left(1-\frac{WR}{Et}\right)[\alpha(1-\mu^2)+(1+\mu)^2]+\alpha+1+\mu\right\}.$$

Equation (32) indicates that solutions, different from zero, exist only if

$$W=W_c=\frac{\dfrac{Et}{R\alpha^2}+\dfrac{EI}{R^3(1-\mu^2)}\left[N^2\{N^2\lambda^2-\mu(\lambda-1)-1\}-\dfrac{\alpha+1+\mu}{\lambda\alpha}\left[N^2\{1+(\lambda-1)(2-\mu)\}-1\right]\right]}{F}.\quad(33)$$

As the uniform external pressure on a round cylinder increases from zero to the value W, the cylinder remains round and in stable equilibrium until W reaches the critical value W_c. At that pressure small variations in the internal forces f, g, h, and j become possible with indeterminate deflections of the cylinder from the round. The boundary values for displacements at the ends come into effect analytically only at the critical load. Actually, on account of the bulkheads (Figs. 12 and 20) the values of z and v at the ends are approximately zero during the whole range of values of W from zero to W_c.

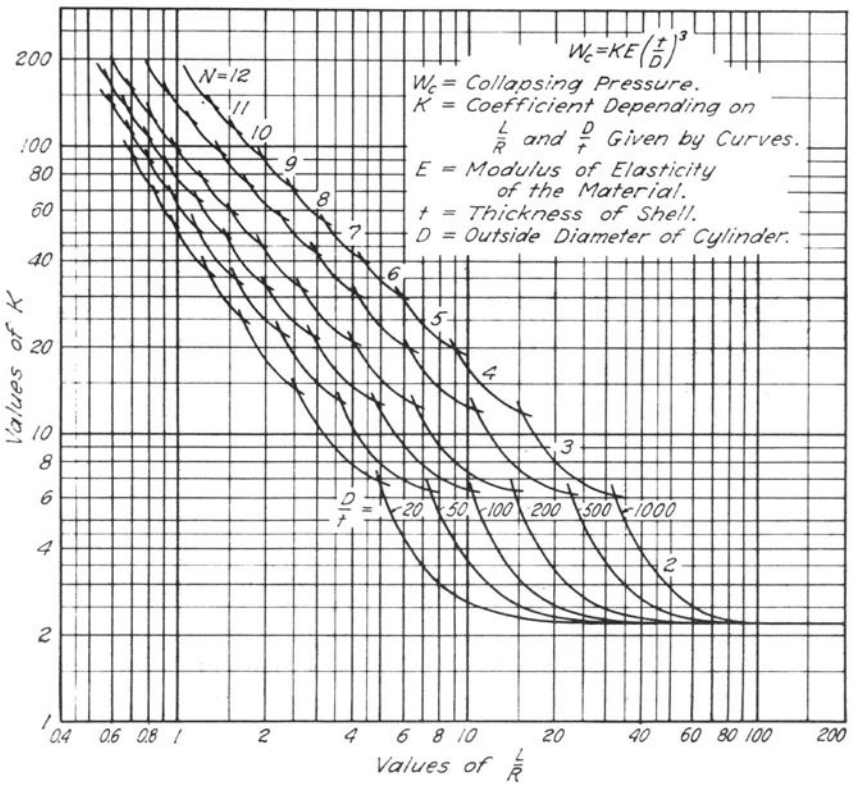

FIG. 4. COLLAPSE-COEFFICIENTS; ROUND CYLINDERS WITH PRESSURES ON SIDES ONLY, EDGES SIMPLY SUPPORTED; $\mu = 0.30$

Since $I = \frac{t^3}{12}$ and $R = \frac{D}{2}$, Equation (33) may be written as

$$W_c = K_1 E \frac{t^3}{D^3} + K_2 E \frac{t}{D} \tag{34}$$

in which

$$K_1 = \frac{2}{3} \frac{N^2\{N^2\lambda^2 - \mu(\lambda-1) - 1\} - \frac{\alpha+1+\mu}{\alpha\lambda}[N^2\{1+(\lambda-1)(2-\mu)\}-1]}{F(1-\mu^2)} \tag{35}$$

$$K_2 = \frac{2}{\alpha^2 F}. \tag{36}$$

For the range of values D/t and L/R considered in this bulletin, F may be approximated by $N^2 - 1$. In order to plot values which give comparisons for various values of N, Equation (34) is written as

$$W_c = \left(K_1 + K_2 \frac{D^2}{t^2}\right) E \frac{t^3}{D^3} = KE\left(\frac{t}{D}\right)^3. \tag{37}$$

This form of the equation is convenient to use, whether the values of K be plotted in the form of charts, or arranged in tabular form.

Equation (37) gives the uniform external pressure at which a round cylinder may collapse into N lobes. The number of lobes giving the minimum value of W has been found by plotting curves for K and L/R for various values of D/t and N. Figure 4 shows a family of K-curves for $\mu = 0.30$. The curves are shown only in the region of the minimum value of K.

(b) *Edges of Shell at Ends Fixed.*—Boundary conditions for this case are $z = 0$, $\frac{\partial z}{\partial y} = 0$, $\frac{\partial v}{\partial \theta} = 0$ for all values of θ at $y = \pm\frac{L}{2}$. From symmetry and continuity, $\frac{\partial z}{\partial y} = 0$ for all values of θ at $y = 0$ and $\frac{\partial z}{\partial \theta} = 0$ for all values of y when $\theta = 0$. A solution of Equations (23), (24), (25), and (26) satisfying these boundary conditions is

$$\begin{aligned} z &= A \cos N\theta \cos \frac{\pi y}{aL} + Ac \cos N\theta \cosh \frac{\pi y}{aL} \\ v &= B \sin N\theta \cos \frac{\pi y}{bL} + Bc \sin N\theta \cosh \frac{\pi y}{bL}. \end{aligned} \tag{38}$$

From the boundary conditions and Equations (38) a relation between a and b is found,

$$\frac{1}{a} \tan \frac{\pi}{2a} + \frac{1}{b} \tanh \frac{\pi}{2b} = 0. \tag{39}$$

The curves in Fig. 5a show the relation of $\frac{1}{a} \tan \frac{\pi}{2a}$ to a and $\frac{1}{b} \tanh \frac{\pi}{2b}$ to b. Values of a and b have been chosen from these curves so that Equation (39) is satisfied. The corresponding relation between a and b is shown in Fig. 5b.

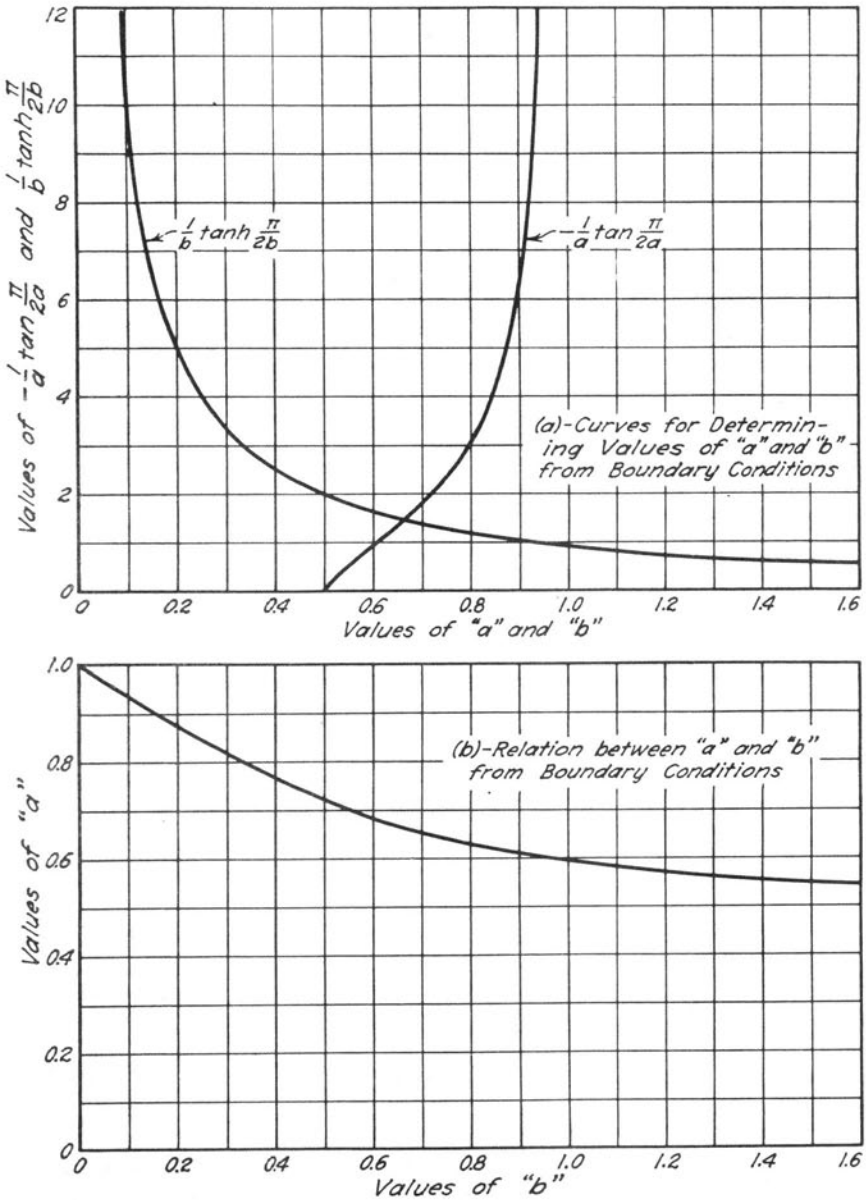

FIG. 5. CURVES FOR DETERMINING a-b RELATION

From Equation (23) it follows that $f(y, s)$ has the form

$$f(y, s) = D \cos N\theta \left[\cos \frac{\pi y}{aL} + d \cosh \frac{\pi y}{bL} \right]$$

and from Equation (24) it follows that

$$g(y, s) = H \cos N\theta \left[\cos \frac{\pi y}{aL} + h \cosh \frac{\pi y}{bL} \right].$$

Substituting the solutions (38) and the derivatives of f and g into Equations (23), (24), (25), and (26), and eliminating all constants except A and Ac, it is found that

$$\begin{aligned}
&\left[\frac{Et}{R^2\alpha_1^2} + \frac{EI}{R^4(1-\mu^2)} \left[N^2 \{ N^2\lambda_1^2 - \mu(\lambda_1 - 1) - 1 \} \right. \right. \\
&\qquad \left. - \frac{\alpha_1 + 1 + \mu}{\alpha_1\lambda_1} [N^2 \{ 1 + (\lambda_1 - 1)(2 - \mu) \} - 1] \right] \\
&\qquad \left. - \frac{W}{R} F_1 \right] A \cos N\theta \cos \frac{\pi y}{aL} + \left[\frac{Et}{R^2\alpha_2^2} \right. \\
&\qquad + \frac{EI}{R^4(1-\mu^2)} \left[N^2 \{ N^2\lambda_2^2 + \mu(\lambda_2 + 1) - 1 \} \right. \\
&\qquad \left. + \frac{\alpha_2 - 1 - \mu}{\alpha_2\lambda_2} [N^2 \{ 1 - (\lambda_2 + 1)(2 - \mu) \} - 1] \right] \\
&\qquad \left. - \frac{W}{R} F_2 \right] Ac \cos N\theta \cosh \frac{\pi y}{bL} = 0 \qquad (40)
\end{aligned}$$

in which

$$\alpha_1 = \frac{N^2a^2L^2}{\pi^2R^2} + 1, \qquad \lambda_1 = \frac{\pi^2R^2}{N^2a^2L^2} + 1,$$

$$\alpha_2 = \frac{N^2b^2L^2}{\pi^2R^2} - 1, \qquad \lambda_2 = \frac{\pi^2R^2}{N^2b^2L^2} - 1$$

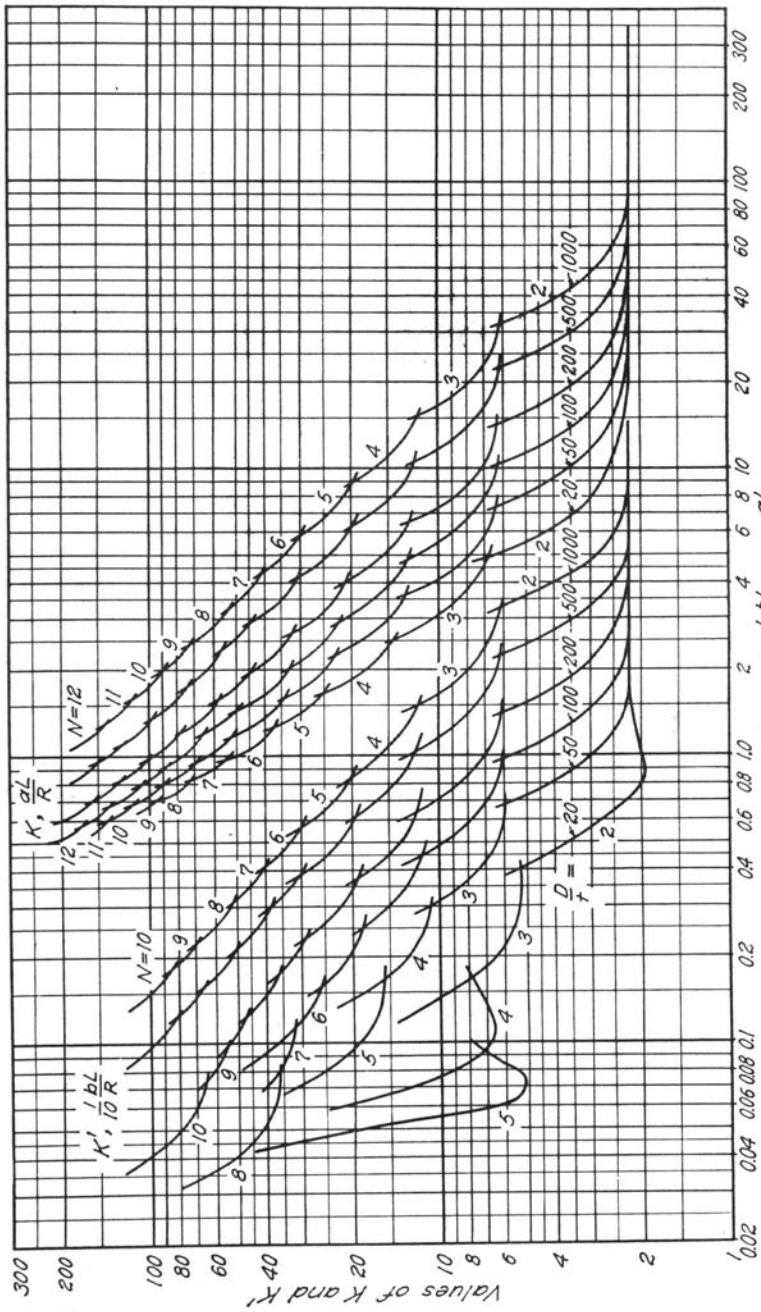

FIG. 6. GRAPHS FOR DETERMINING a/b RATIOS, FIXED EDGES

$$F_1 = N^2 - 1 + \frac{1}{\alpha_1^2} - \frac{\mu}{\alpha_1\lambda_1} - \frac{I}{R^2(1-\mu^2)t\lambda_1\alpha_1}\left[N^2\{1+(\lambda_1-1)(2-\mu)\}-1\right]\left[\alpha_1+1+\mu+\left(1-\frac{WR}{Et}\right)\{\alpha_1(1-\mu^2)+(1+\mu)^2\}\right]$$

$$F_2 = N^2 - 1 + \frac{1}{\alpha_2^2} - \frac{\mu}{\alpha_2\lambda_2} + \frac{I}{R^2(1-\mu^2)t\lambda_2\alpha_2}\left[N^2\{1-(\lambda_2+1)(2-\mu)\}-1\right]\left[\alpha_2-1-\mu+\left(1-\frac{WR}{Et}\right)\{\alpha_2(1-\mu^2)-(1+\mu)^2\}\right].$$

In this equation the coefficients of $A\cos N\theta\cos\frac{\pi y}{aL}$ and the coefficients of $Ac\cos N\theta\cosh\frac{\pi y}{bL}$ must vanish separately if the equation is to hold for all values of θ and y. From this condition two equations are obtained both containing W. Since W can have only one value, another relation between a and b results.

The value of W obtained from the coefficient of the first term of Equation (40) will again be expressed as W_c and is the same as that obtained for simply supported edges except that L is replaced by aL in the values α and λ. Equation (33) may therefore be used. The values of K have been replotted in Fig. 6 with aL/R as abscissae.

The expression for W_c obtained from Equation (40) by equating the coefficient of the second term to zero is

$$W_c = E\left(K_1' + K_2'\frac{D^2}{t^2}\right)\frac{t^3}{D^3} = K'E\left(\frac{t}{D}\right)^3 \tag{41}$$

in which

$$K_1' = \frac{2}{3}\,\frac{N^2\{N^2\lambda_2^2+\mu(\lambda_2+1)-1\}+\frac{\alpha_2-1-\mu}{\alpha_2\lambda_2}[N^2\{1-(\lambda_2+1)(2-\mu)\}-1]}{(1-\mu^2)F_2} \tag{42}$$

and

$$K_2' = \frac{2}{\alpha_2^2 F_2}. \tag{43}$$

Values of K' and $\frac{1}{10}\frac{bL}{R}$ are shown in Fig. 6. The arbitrary value 1/10 used in the abscissae scale moves the curves to the left to avoid confusion from overlapping curves.

For every aL/R there exists a corresponding bL/R so that $K' = K$. Then from values of aL/R and bL/R obtained from Fig. 6, ratios of a/b are found.

Finally, the determination of a is obtained as the ordinate of the curve in Fig. 5b at its intersection with a line through the origin whose slope is a/b as found in Fig. 6. Knowing the value of a for values of aL/R the value of L/R is readily obtained. The values of K from the aL/R curves are then replotted with L/R, thus giving K curves for cylinders with fixed edges, (Fig. 7).

(c) *Edges of Shell at Ends Restrained.*—In actual practice it very rarely happens that the edges of the shell at the ends of the cylinder are either simply supported or completely fixed. The shell is usually attached to a stiffening ring or bulkhead which offers some restraint but does not completely fix the edges. For such cases, the degree of restraint which exists is best determined from tests on actual cylinders.

13. *Pressure Applied to Sides and Ends.*—For this case the value of the longitudinal force P_y is expressed as

$$P_y = \frac{-WR}{2} + g\,(y, s).$$

Equation (19) then becomes

$$\frac{EI}{1-\mu^2}\left[\frac{\partial^4 z}{\partial y^4} + \frac{\mu}{R^2}\frac{\partial^2 z}{\partial y^2} + \frac{2}{R^2}\frac{\partial^4 z}{\partial \theta^2 \partial y^2} + \frac{1}{R^4}\frac{\partial^2 z}{\partial \theta^2} + \frac{1}{R^4}\frac{\partial^4 z}{\partial \theta^4}\right] + \frac{1}{R} f\,(y, s) = -W\left(\frac{1}{R}\frac{\partial^2 z}{\partial \theta^2} + \frac{z}{R} - \epsilon_s\right) - \frac{WR}{2}\frac{\partial^2 z}{\partial y^2}. \tag{44}$$

Equations (24), (25), and (26) remain as before.

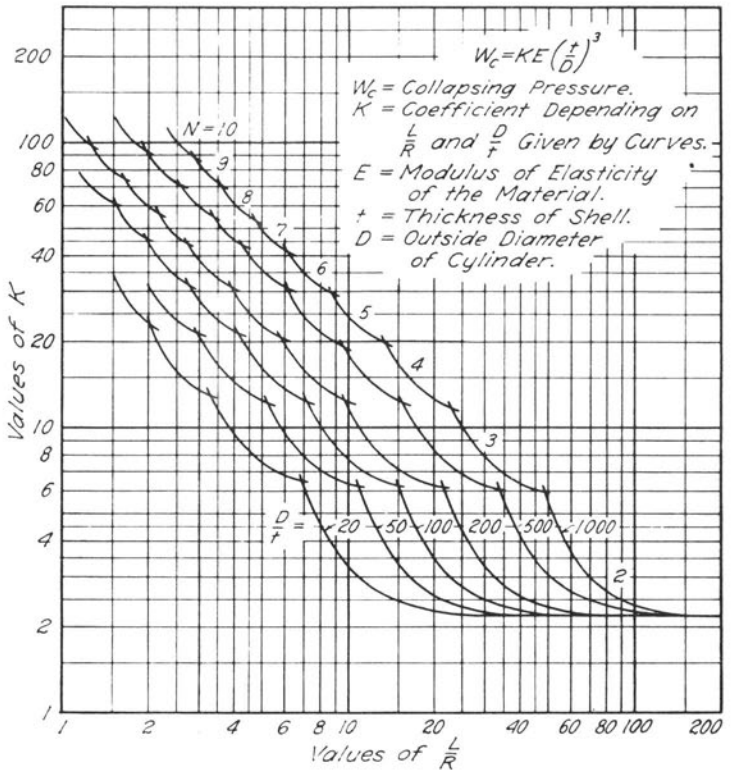

FIG. 7. COLLAPSE-COEFFICIENTS; ROUND CYLINDER WITH PRESSURE ON SIDES ONLY, FIXED EDGES; $\mu = 0.30$

(a) *Edges of Shell at Ends Simply Supported.*—Since the boundary conditions are the same as for lateral pressure only, the solutions (27) are tried. Substituting the values for z and v into Equations (24), (25), and (26), B, C, and D are determined as before. W_c corresponds to the value given by Equation (33), except that the denominator now becomes $F + \frac{\pi^2 R^2}{2L^2}$. The collapsing pressure may again be written in the form of Equation (37), K_1 and K_2 being replaced by K_1'' and K_2''. The values of K_1'' and K_2'' are readily obtained from the former values K_1 and K_2 by multiplying each value by the ratio r of the denominator, F, in Equation (33) to the new denominator,

$$r = \frac{F}{F + \frac{\pi^2 R^2}{2L^2}}. \tag{45}$$

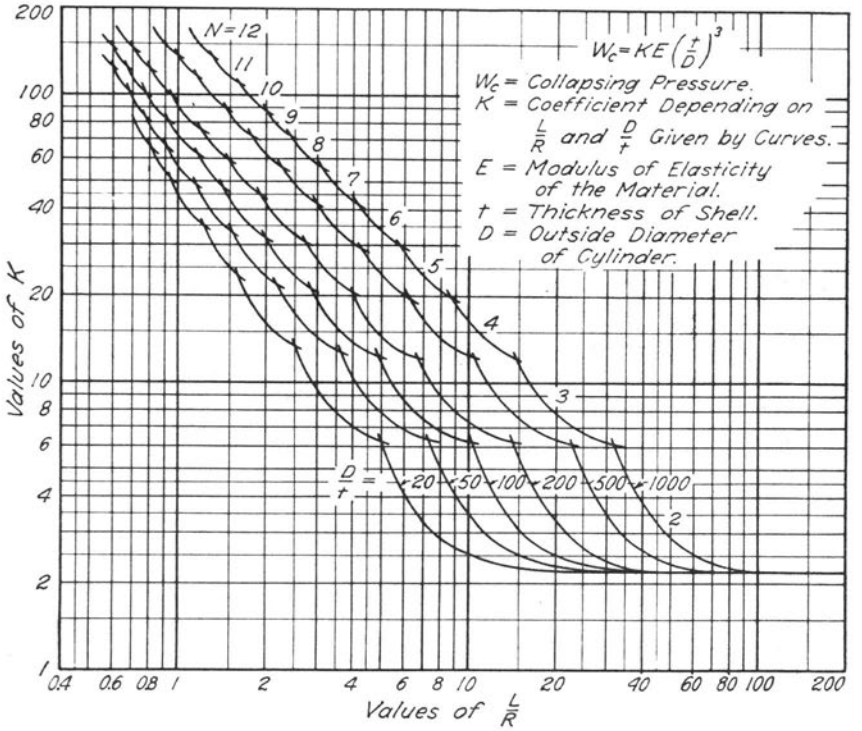

FIG. 8. COLLAPSE-COEFFICIENTS; ROUND CYLINDER WITH PRESSURE ON SIDES AND ENDS, EDGES SIMPLY SUPPORTED; $\mu = 0.30$

The new values, K, differ from the previous values by amounts depending on L/R, and consequently lead to a different range of values of L/R for which any given number of lobes, N, gives rise to a minimum collapsing pressure. Curves for K (Fig. 8) have been plotted to indicate the ranges in which each value of N gives a minimum collapsing pressure for this new condition. Only those portions of the curves, for the various values of N, which give minimum values of collapsing pressure, are shown.

(b) *Additional End Load.*—If a uniform axial longitudinal load P per linear unit of circumference is applied to the cylinder in addition to the external pressure W, the value of P_y becomes

$$P_y = \frac{-WR}{2} - P + g\,(y, s).$$

The right side of Equation (44) then becomes

$$-W\left(\frac{1}{R}\frac{\partial^2 z}{\partial\theta^2}+\frac{z}{R}-\epsilon_s\right)-\frac{WR}{2}\frac{\partial^2 z}{\partial y^2}-P\frac{\partial^2 z}{\partial y^2}.$$

The new value of r corresponding to Equation (45), represented by r' is

$$r'=\frac{F}{F+\dfrac{\pi^2R^2}{2L^2}+\dfrac{P}{W_cR}\dfrac{\pi^2R^2}{L^2}}. \tag{46}$$

The value of P in this equation may be either positive (compressive load) or negative (tensile load). In general the effect of compressive loads will be to reduce the collapsing pressure and of tensile loads to increase the collapsing pressure within the elastic range of the material. For long cylinders of relatively large ratios of diameter to thickness, however, this effect is generally small. Because of the general nature of the longitudinal force, P, curves for K cannot be computed until specific values are assigned to the force P.

(c) *Edges of Shell at Ends Fixed.*—The boundary conditions are the same as for lateral pressures only, and all that is required is to multiply each value of the collapsing pressure by the ratio, r, from Equation (45). This, however, should be done for values of aL and bL, but, since each term will be multiplied by the same r for a given N and L/R, it follows that the ratios of a/b will be the same as for lateral pressures only. And since the boundary relationship, as expressed by Equation (39), will not be changed, the same values of a will be obtained. Therefore it is sufficient to multiply each final K' by its corresponding value of r and the new values, K'', will be obtained. Here again the range of L/R for which a given N will give a minimum collapsing pressure is different from that for the case of lateral pressure only.

Figure 9 shows the value of K for pressure applied to sides and ends. Again only those portions of the curves for the various values of N which give minimum values of collapsing pressure are shown.

(d) *Edges of Shell at Ends Restrained.*—Here again interpolation between the two limiting cases may be made for various amounts

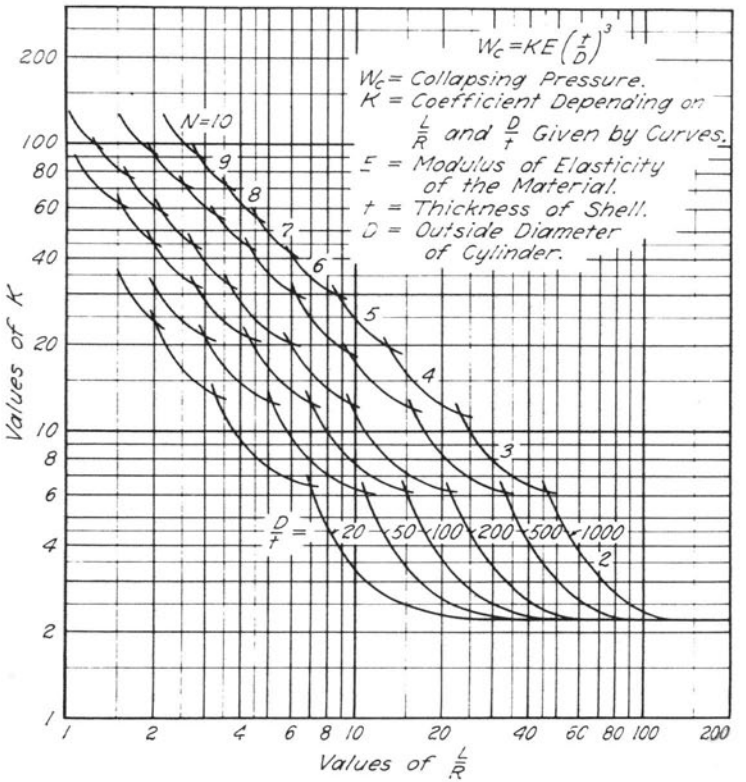

FIG. 9. COLLAPSE-COEFFICIENTS; ROUND CYLINDER WITH PRESSURE ON SIDES AND ENDS, FIXED EDGES; $\mu = 0.30$

of restraint obtained in actual practice. The actual amount of restraint for various standard types of stiffeners and methods of framing may be determined from tests designed to give this information.

14. *Pressure on Ends Only.*—If there is a uniform longitudinal pressure P per unit of length of circumference but no lateral pressure on the cylinder, the same general differential equations (Section 11) may be used to determine the load at which the shell becomes unstable.

W is now zero, $P_s = 0 + f(y, s)$ and $P_y = -P + g(y, s)$.

Tests have shown that the cylinder may buckle so that the wave length of the buckle is very much shorter than the length of the tube. The solutions, z and v for this form of buckling may be taken the

same as in Section 13, the value of L being replaced by L_o, the length of one wave. The value of C in the function $f(y, s)$ is

$$\frac{C}{A} = \frac{Et}{R\alpha_o^2} - \frac{EI}{R^3(1-\mu^2)}\left[N^2\{1+(\lambda_o-1)(2-\mu)\}-1\right]\frac{\alpha_o+1+\mu}{\alpha_o\lambda_o}\left(1+\mu\frac{PR}{Et}\right)$$

where

$$\alpha_o = \frac{N^2L_o^2}{\pi^2R^2} + 1 \qquad \text{and} \qquad \lambda_o = \frac{\pi^2R^2}{N^2L_o^2} + 1.$$

The value of P which makes the coefficients of the term $\cos N\theta \cos\frac{\pi y}{L_o}$ vanish is the force at which neutral equilibrium may prevail, and is considered as the collapsing force, P_c. The value for P_c is

$$P_c = \frac{\dfrac{Et}{\alpha_o\lambda_o} + \dfrac{EI}{R^2(1-\mu^2)}(\alpha_o-1)\left[N^2\{N^2\lambda_o^2-\mu(\lambda_o-1)-1\} - \dfrac{\alpha_o+1+\mu}{\alpha_o\lambda_o}[N^2\{1+(\lambda_o-1)(2-\mu)\}-1]\right]}{N^2+\dfrac{\mu I}{R(1-\mu^2)t\lambda_o^2}(\alpha_o+1+\mu)\left[N^2\{1+(\lambda_o-1)(2-\mu)\}-1\right]}. \quad (47)$$

P_c may be expressed in terms of the average longitudinal compressive stress, S_c, as

$$P_c = S_ct. \quad (48)$$

With $I = \frac{1}{12}t^3$, $\mu = 0.30$ and small values of t/R

$$S_c = 0.6E\frac{t}{R}. \quad (49)$$

This equation corresponds to results obtained by other investigators.[13]

The effect of finite initial deflections on the critical load has been studied by L. H. Donnell.[11] The extent to which fabrication affects the critical load is shown by the tests performed by Wilson and Newmark[10] on actual stand pipe sections. They found that the critical loads averaged about one-fourth of the theoretical values for round cylinders.

IV. Round Cylinders Stiffened With Rings

15. *Shell Round at Each Ring.*—If the rings are sufficiently stiff to hold the shell essentially round at each stiffener, the shell may be considered as divided into a series of short shells whose length is the distance between rings. The size of ring necessary to hold the shell against buckling at the ring may be determined as follows:

If the section of the shell between stiffening rings will withstand an external pressure W_s, the stiffened shell as a whole should be able to withstand an equal pressure. If several stiffeners are used or the cylinder is long, the effect of the conditions of the ends of the shell upon the size of the rings will be very small. Therefore, the flexural rigidity of the combined stiffener and shell in the circumferential direction should be the same as that of a long cylinder which would support an external pressure W_s.

If the thickness of the long cylinder which just supports W_s is denoted by t_s, then from Equation (37)

$$W_s = KE\frac{t_s^3}{D^3}. \tag{50}$$

For long cylinders, K_2 approaches zero, and the value of K is approximately $\dfrac{2}{(1-\mu^2)}$.

This value substituted into Equation (50) gives

$$Et_s^3 = \frac{W_s D^3(1-\mu^2)}{2}. \tag{51}$$

The flexural rigidity of this long cylinder, for a length of shell equal to the stiffener spacing, L_s, is

$$EI_s = \frac{Et_s^3 L_s}{12(1-\mu^2)}. \tag{52}$$

Combining Equations (51) and (52), the flexural rigidity of a cylinder necessary to withstand an external pressure, W_s, becomes

$$EI_s = \frac{W_s D^3 L_s}{24}. \tag{53}$$

Since the stiffened shell must carry a pressure, W_s, the flexural rigidity of the combined stiffener and shell must be the same as that of the long cylinder. The flexural rigidity of the combined stiffener and shell may be closely approximated by the product of the modulus of elasticity and the sum of an equivalent moment of inertia of the stiffener and a portion of the shell wall which may be considered to act with it plus the moment of inertia of the remainder of the shell wall.

V. Cylinders Slightly Out-of-Round

16. *Out-of-Round Unstiffened Cylinders.*—Regardless of how much care is taken in the manufacture of tubes, pipes, or cylinders in general, there are always slight variations from the round which in general follow a random distribution. The degree to which the accidental initial conformation agrees with the conformation of the round cylinder at collapse determines the suddenness of the failure; close agreement causing a gradual collapse.

Assume that correspondence exists between the initial "out-of-roundness" and the "normal" conformation of the round shell at collapse. For the case of simply supported edges the normal conformation of a round cylinder in the state of neutral equilibrium is given by (Section 12a—displacement v may be neglected)

$$z = A \cos \frac{\pi y}{L} \cos N\theta.$$

The initial out-of-roundness is assumed of the same form

$$z_o = A_o \cos \frac{\pi y}{L} \cos N\theta.$$

The total deflection is

$$z + z_o = (A + A_o) \cos \frac{\pi y}{L} \cdot \cos N\theta. \tag{54}$$

Referring to Equation (23) it is noted that the terms on the left side depend upon the change in shape z, whereas the terms on the right side depend upon the total deviation from the round cylinder, $z + z_o$.

From Equations (24), (25), and (26) the values of $f(y, s)$ and $g(y, s)$ will be the same as for the round cylinder. If the value of $f(y, s)$ is substituted into Equation (23), the general expression for a cylinder with simply supported edges will be the same as Equation (32), except that the right side of the equation will have the term $(A + A_o)$ instead of A. If both sides of the equation are divided by $A \cos \frac{\pi y}{L} \cos N\theta$, the value of A is found to be

$$A = \frac{WA_o}{W_c - W}. \tag{55}$$

This expression for the maximum deflection of a slightly out-of-round cylinder is of the same type as Fidler's[26] expression for the deflection of slightly imperfect columns, and agrees with the results of Westergaard in a general consideration of the buckling of elastic structures.[20]

If there is an "out-of-roundness" which does not agree with the normal pattern of collapse, i.e., with the value of N which gives a minimum pressure for a perfect cylinder, the value of A_o may increase appreciably when the number of lobes is different by 1 or 2. Refer to Figs. 4, 7, 8, and 9, and note that in cases where N is large the collapsing pressure for a round cylinder buckling into one more or less lobes than the number giving a minimum will be only slightly larger than the minimum. Consequently it is possible that the increase in A_o resulting from a better fit with "out-of-roundness" will more than offset the increase in W_c produced by the change in number of lobes, with the result that the cylinder may collapse into a number of lobes different from that indicated for a round tube.

Similar arguments may be applied to the case of fixed or restrained edges.

If the magnitude of the deflection, A, is known, the bending moment can be computed from Equation (8).

$$M_s = \frac{EI}{1 - \mu^2}\left[\frac{N^2 - 1}{R^2} + \mu\frac{\pi^2}{L^2}\right] A \cos N\theta \cos\frac{\pi y}{L}. \tag{56}$$

The maximum value of M_s occurs where $\cos \frac{\pi y}{L} \cos N\theta = 1$, or at the center of a buckle.

The maximum stress, S, in the s direction may be found as the sum of the direct stress, S_1, plus the bending stress S_2. The average direct stress is

$$S_1 = \frac{WR}{t} \tag{57}$$

and the maximum bending stress is

$$S_2 = \frac{M_s t}{2I} = \frac{Et}{2(1-\mu^2)} A \left(\frac{N^2 - 1}{R^2} + \mu \frac{\pi^2}{L^2} \right). \tag{58}$$

In terms of A_o the total maximum stress is

$$S = S_1 + S_2$$

$$= \frac{WR}{t} \left[1 + \frac{EA_o}{2(1-\mu^2)(W_c - W)t} \frac{t^3}{R^3} \left(N^2 - 1 + \mu \frac{\pi^2 R^2}{L^2} \right) \right]. \tag{59}$$

When the maximum stress S reaches a value beyond which plastic action takes place, the value of W_c will decrease, thereby increasing the distortion and stress which in turn causes further plastic action and so on.

It is often desirable to determine the maximum external pressure that can be supported by a vessel with a known initial radial deviation from a round cylinder. Specifications may give limiting permissible values of initial distortion, and at the same time require that no permanent set occur. To meet this condition the maximum stress S should not exceed the elastic limit for the particular state of stress existent in the cylinder considered.

Let the allowable stress be $\overline{S}$, and let the value of W corresponding to $\overline{S}$ be $\overline{W}$. Then Equation (59) may be written as

$$\overline{S} = \frac{\overline{W}R}{t} \left[1 + \frac{EA_o}{2(1-\mu^2)(W_c - \overline{W})t} \frac{t^3}{R^3} \left(N^2 - 1 + \mu \frac{\pi^2 R^2}{L^2} \right) \right]. \tag{60}$$

Values of $\overline{W}$ may readily be computed by trial and error if Equation (60) is written in the form

$$\overline{W} = \frac{2\overline{S}\frac{t}{D}}{1 + \frac{4A_o}{t}\frac{E\left(N^2 - 1 + \mu\frac{\pi^2R^2}{L^2}\right)\frac{t^3}{D^3}}{(1-\mu^2)(W_c - \overline{W})}}. \tag{61}$$

This equation shows that the values of L/R and D/t as well as A_o/t and $\overline{S}$ are necessary to determine the effect of out-of-roundness in a cylinder subjected to external pressure. It also shows that if W_c causes an average stress which is small compared to $\overline{S}$, the load $\overline{W}$ necessary to produce the stress $\overline{S}$ will be close to W_c for nearly all reasonable values of A_o/t.

In order to obtain the maximum pressure which such an "out-of-round" cylinder can carry, the modulus of failure, S_u, may be used instead of $\overline{S}$ and the value of W_c reduced as described in Section (18).

17. *Out-of-Round Cylinders Stiffened With Rings.*—Stiffening rings should have sufficient rigidity to retain their shape regardless of whether the shell buckles between them or not. The deviations from true circularity of the cylinder will be most severe when the stiffener tends to flatten, i.e., forming two lobes. The deflection of the stiffener may then be represented by

$$z_{st} = A \cos 2\theta. \tag{62}$$

Because of the general applicability of Equation (55) the maximum deflection A may be found from this equation, where W_c is interpreted as being the pressure at which the stiffener becomes unstable. The bending moment in the stiffener is obtained from Equation (8), with μ assumed equal to zero.

$$M_{st} = EI_s\frac{3A_o}{R_s^2}\frac{W}{W_c - W}\cos 2\theta. \tag{63}$$

R_s is the radius from the center of the cylinder to the centroid of a right section of the stiffener and the plate effective with it. The stress in the stiffener is the combined direct and bending stress.

VI. Extension to Plastic Action

18. *Cylinders in Which Stresses Are Beyond Elastic Range.*—In many instances cylinders do not collapse until the stress in the shell wall exceeds the elastic limit of the material.

In 1889 Engesser[27] proposed using the actual tangent modulus of elasticity as determined from stress-strain curves of the material for the effective modulus. Later work by A. Considère[28] and Th. v. Kármán[29] has shown that by the introduction of a double modulus the theory is in better agreement with tests on straight columns axially loaded. A summary by Osgood[30] gives results obtained by applying v. Kármán's principles to columns of various structural sections. The double modulus theory makes use of the modulus for decreasing stresses, which is taken equal to E, for the elastic range, and the modulus for increasing stresses in the plastic range. The latter, E_1, is the tangent modulus at the average stress in the member considered.

The "effective" modulus of elasticity for columns with rectangular sections, according to the double modulus theory, is

$$E' = \frac{4E_1}{1 + \sqrt{\left(\frac{E_1}{E}\right)^2}}. \tag{64}$$

The derivation of Equation (64) is based upon the assumption that the column is perfectly straight to begin with, and remains so until buckling occurs; at this time the stress on one side of the column rapidly increases while on the other side it rapidly decreases. If the column is slightly crooked initially, the phenomenon of sudden buckling, as considered by Considère and v. Kármán, does not occur. Westergaard and Osgood[31] have shown how much effect a slight deviation from perfection can have on the load-carrying capacity of steel columns. In view of these considerations the observed critical loads for columns might well be expected to be somewhat below that given by the double modulus theory.

Any tendency of the material to creep would also tend to reduce the effective modulus under sustained load. In tests for stability, the specimens often carry a given load for an appreciable time (as long as several hours or more) and then buckle without an increase in load.

Since the tangent modulus at the average stress for inelastic

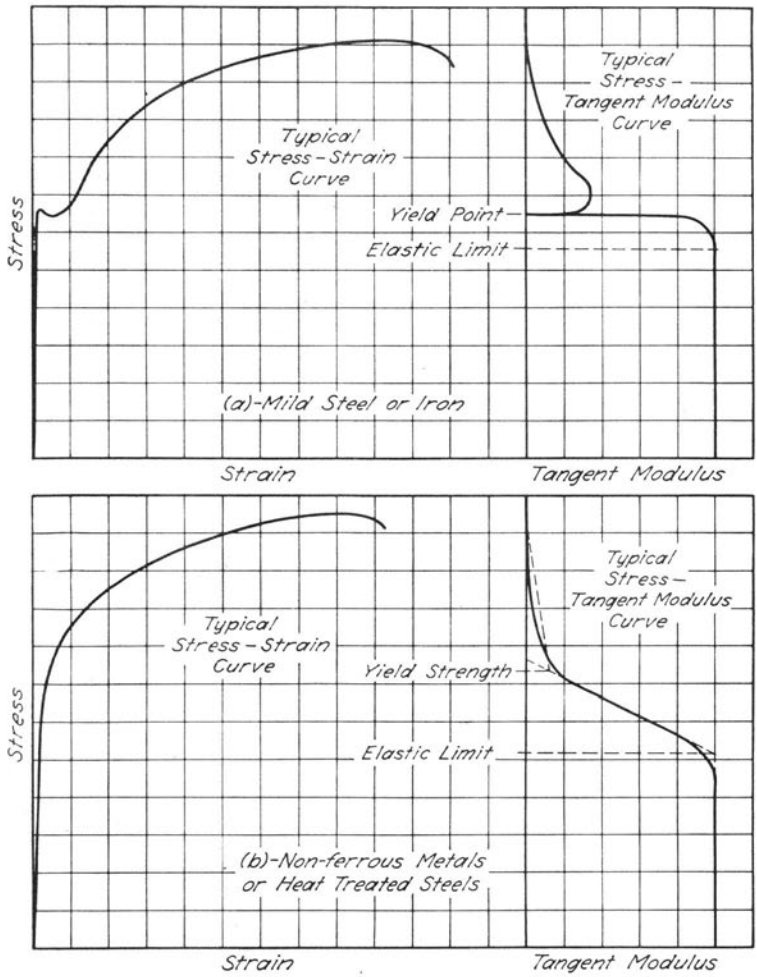

FIG. 10. TYPICAL STRESS–TANGENT MODULUS CURVES

action is always less than the effective modulus according to Equation (64) it is proposed to formulate expressions for the tangent modulus for use as the effective modulus. Three cases may be distinguished, (1) the average stress is between the elastic limit and the yield strength, (2) the average stress is between the yield strength and the ultimate strength and (3) the average stress is less than the proportional limit with the maximum stress considerably above the elastic limit.

For the first two cases the tangent modulus at the average stress

is approximately equal to the average tangent modulus for the normal stress distribution over the section. The average tangent modulus is defined as that modulus which is in accord with the statical conditions as to the resultant stress and the moment thereof.

Case 1. The average stress S_1 is between the elastic limit* Q and the yield strength S_y. Figure 10 shows that the stress-modulus curve for the aluminum alloy may be simplified as indicated by the dotted lines. From the geometry of this figure the following expression for the effective modulus is obtained,

$$E' = E\left[1 - (1 - \beta)\frac{S_1 - Q}{S_y - Q}\right]. \tag{65}$$

β is the ratio of the tangent modulus at S_y to the initial tangent modulus E.

Case 2. The average stress, S_1, is between the yield strength, S_y, and the ultimate strength, S_u. The effective modulus is

$$E' = \beta E\left[1 - \frac{S_1 - S_y}{S_u - S_y}\right]. \tag{66}$$

Case 3. Where the average stress is less than the proportional limit but, because of eccentricities, the maximum stress in the shell exceeds the elastic limit, an empirical expression for the effective modulus has been found to be satisfactory for columns. This expression is proposed for cylinders which come under this case. The formula† is

$$E' = E\left[1 - \frac{1}{4}\left(\frac{S - Q}{S_u - S_1}\right)^2\right]. \tag{67}$$

S is the maximum stress in the shell (direct and bending).

For round cylinders in which the stresses are above the proportional limit of the material, the collapsing pressure is now written

$$W_c = KE'(t/D)^3. \tag{68}$$

It should be remembered in connection with the use of the coefficients, K, that they are derived for the case of linear elastic action.

*The elastic limit is taken as 1.1 times the proportional limit as determined by Tuckerman.[32]
†The formula (67) is based on tests made at the Research Laboratories of the Aluminum Company of America.

In the plastic range, however, if the same values of K are used, there will be a discrepancy because of the fact that stresses are not proportional to the distance from the neutral surface, and that Poisson's ratio is not the same as in the elastic range. Experiments indicate, however, that in the plastic range the approximations are sufficiently close within certain limits of t/D and L/R.

The value of W_c obtained from Equation (68) may be used in Equation (61), together with the value of E' instead of E, to give the allowable pressure for slightly out-of-round cylinders.

Attention is called to the fact that the existence of longitudinal stresses affects the nature of plastic deformation both as to the magnitude of the stress at which plastic action starts and as to the characteristic shape of the stress-strain curve as plastic action progresses. Therefore, for combined stresses the value of the effective reduced modulus for combined stresses may be significantly different and start at significantly different stresses than for a single direct stress.

The resultant effects of superimposed longitudinal tension or compression upon the collapsing pressure of thin cylinders therefore requires two-fold consideration; its effects upon the inherent stability of the cylinder as discussed in Section 13b and its effects upon the inception and progress of plastic deformation in the material of which the cylinder is made.

Studies of effects of biaxial stress upon the stress-strain characteristic of materials have been made by Lode[36], Nadai[37], Marin and Stanley[38], Lessells and McGregor[39], and others.

The experimental results obtained by these investigators seem to justify the method used by Holmquist and Nadai[40] in accounting for the effects of biaxial stress. This method gives the stress at inception of plastic action as

$$S_1^2 - S_1 S_p + S_p^2 = S_y^2. \tag{69}$$

VII. Experimental Work

19. *Effects Considered.*—In reports of previous experimental investigations of the collapse of thin-walled cylinders there seems to be little information on the relative effects of pressures applied on both the sides and ends of vessels as compared with pressure applied on the sides only. Also, effects due to edge restraint and "out-of-roundness" on the strength of a given cylinder have not been adequately considered. These effects were taken into account in planning the following tests.

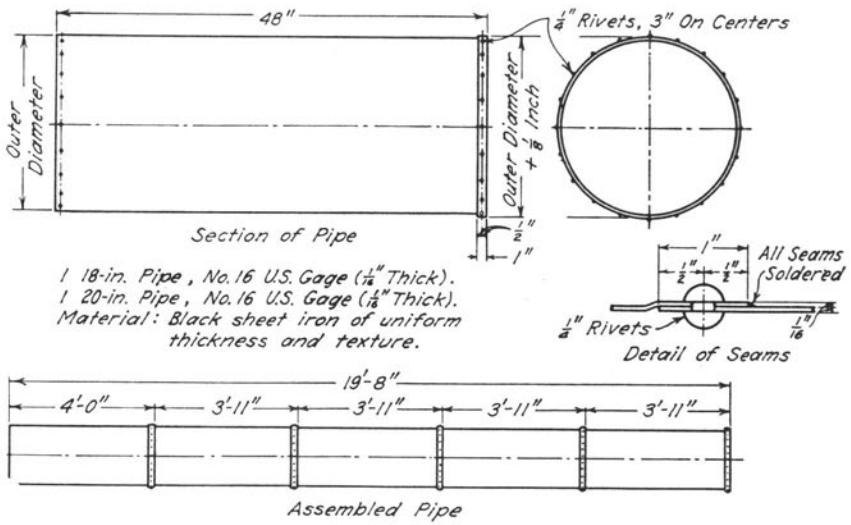

FIG. 11. THIN-WALLED PIPE FOR COLLAPSE TEST

Two series of tests were made by the author, one at the University of Illinois during 1928-1929 and the other at the Aluminum Research Laboratories during 1931-1933.

A. Tests at the University of Illinois

20. *Object of Tests.*—The tests were made on two built-up steel pipes for the general purpose of studying the behavior of shells at or near the point of collapse, and to give validity to some of the fundamental assumptions stated in the analysis.

21. *Specimens.*—Two pipes approximately 20 ft. long, one 20 in. in diameter and the other 18 in. in diameter, were made from 16-gage (0.063 in. thick) black sheet iron which was rolled into sections of 4-ft. length, and fastened together longitudinally by riveted and soldered lap joints. One end of each section was belled so as to receive the end of the adjacent section, thereby making a circumferential lap joint. These joints were also riveted and soldered so as to make them airtight. Figure 11 shows details of the tubes as designed.

In the first set of tests the smaller pipe was placed inside the larger one, and the ends of the opening between the pipes sealed by means of a reinforced concrete ring 3 inches thick, Fig. 12. The ring also served to center the smaller pipe in the larger one. The

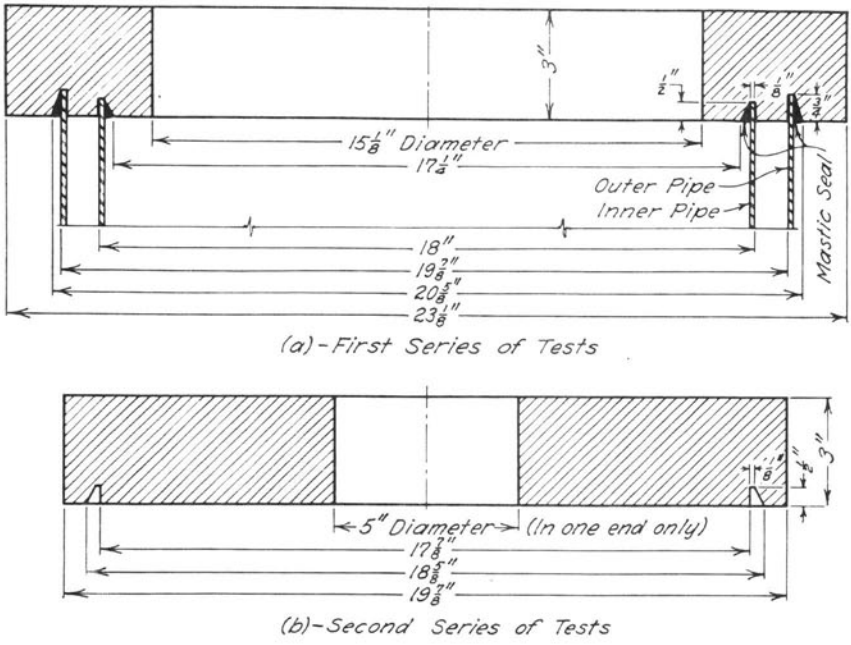

FIG. 12. SECTION THROUGH IRON-PIPE BULKHEAD

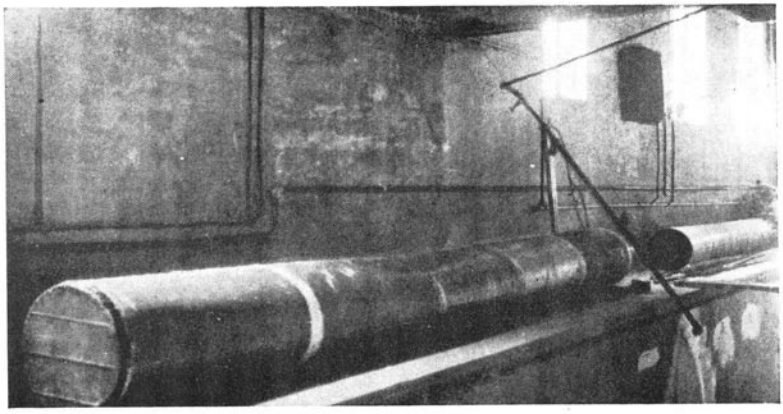

FIG. 13. VIEW OF 20-INCH STEEL PIPE AFTER COLLAPSE

end of each pipe was supported and sealed in a V-shaped notch which offered little restraint against longitudinal tipping of the supported edges. The groove for the inner pipe was less deep than for the outer one, enabling the inner pipe to carry longitudinal pressure. Various

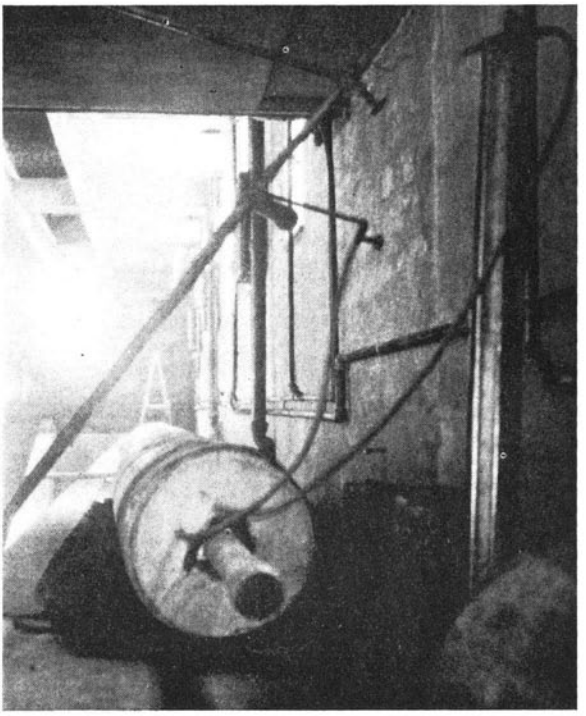

FIG. 14. VIEW OF ADJUSTABLE BULKHEAD, MANOMETER, AIR EJECTION PUMP, 20-INCH STEEL PIPE

sealing materials were tried; the one which gave the best service was a low melting asphalt.

In the second set of experiments each pipe was tested separately and the ends again sealed by means of concrete bulkheads fitting inside the shell and sealed with asphalt. The edges of the shell were supported on the edge of the bulkhead. In this set of tests the end thrust on the bulkhead was carried by a 3-in. cast iron pipe extending through the center of the test pipe. Figure 13 shows the solid concrete bulkhead at one end of the specimen to which the pipe was anchored, and Fig. 14 shows the pipe extending through the bulkhead at the other end of the specimen. A heavy clamp served as a stop for the bulkhead.

22. *Apparatus.*—In the first set of tests the air was pumped out of the space between the pipes by means of an ejector pump, Fig. 13. The diameters of the pipe were measured by a caliper which consisted of a heavy wooden U-frame which had a fixed point attached

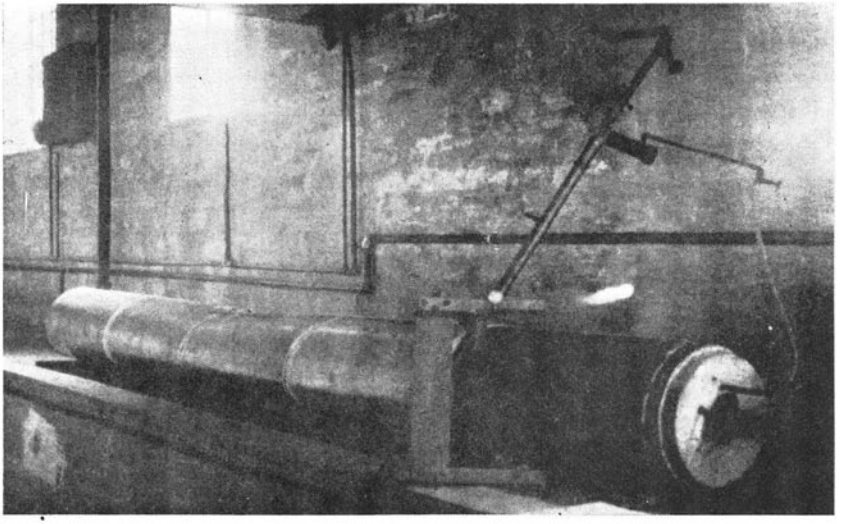

FIG. 15. VIEW OF COLLAPSED 20-INCH STEEL PIPE AND CALIPERS

to the inner side of one leg and a hinged lever on the inner side of the other leg. The lever actuated a dial gage so that when the caliper was placed over the pipe the lever would spring against the pipe, thus giving a reading on the dial. A view of the calipers is shown in Fig. 15. Calibration was made by readings on bars of known lengths. With the calipers differences in diameter of ± 0.005 in. were estimated and readings on a standard length were always duplicated within 0.01 in. The difference in pressure between the air within the shell and the surrounding atmosphere was indicated by a mercury manometer, on which observations were read to the nearest 1/100 in. of mercury (0.005 lb. per sq. in.).

In the first set of tests the inner pipe prevented a radial deformation of the outer pipe of more than one inch. Thus it was possible to retest the outer pipe repeatedly without causing any measurable permanent set. Measurements of the diameter were made on equally spaced diameters at several places along the pipe, both between the circumferential seams and directly over them.

In the second set of tests no preliminary loads were applied, fewer diameter readings were taken, and the pressure was steadily increased until the pipe collapsed.

23. *Discussion of Tests and Results.*—The first set of tests showed that the collapse of an appreciably imperfect tube or cylinder is

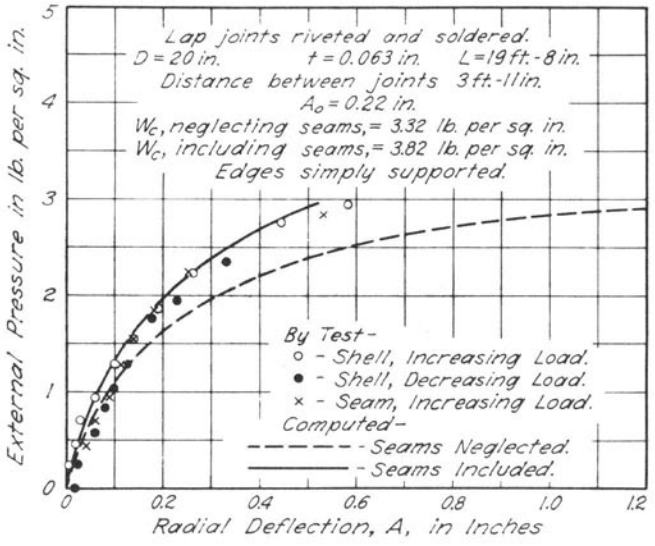

FIG. 16. RADIAL DEFLECTION CURVES—20-INCH STEEL PIPE WITH PRESSURE ON SIDES ONLY; $A_o = 0.22$ INCHES

gradual and not sudden. This phenomenon is similar to the buckling of an eccentrically loaded straight column or a centrally loaded curved column.

Deflections of the twenty-inch pipe in the first set of tests are plotted in Fig. 16. The deflections were measured at a number of positions for zero pressure after the shell had been subjected to an external pressure of about 2 lb. per sq. in. several times, in attempts to obtain a seal that would hold the vacuum constant long enough to obtain a set of readings. Figure 16 shows the curves of radial deflection (taken as one-half of the change in diameter for these tests) for both increasing and decreasing pressures. Collapsing pressures for the shell only (seams neglected) were computed from Equation (37). Since λ is nearly equal to unity for $N \geqq 2$ and values of α and D/t are relatively large, by putting $\lambda = 1$ and neglecting those terms containing α and $(t/D)^2$ which are small compared to unity, the K values in (37) may be simplified to

$$K_1 = \frac{2}{3} \frac{N^2 - 1}{1 - \mu^2}$$

$$K_2 = \frac{2}{\alpha^2(N^2 - 1)}.$$

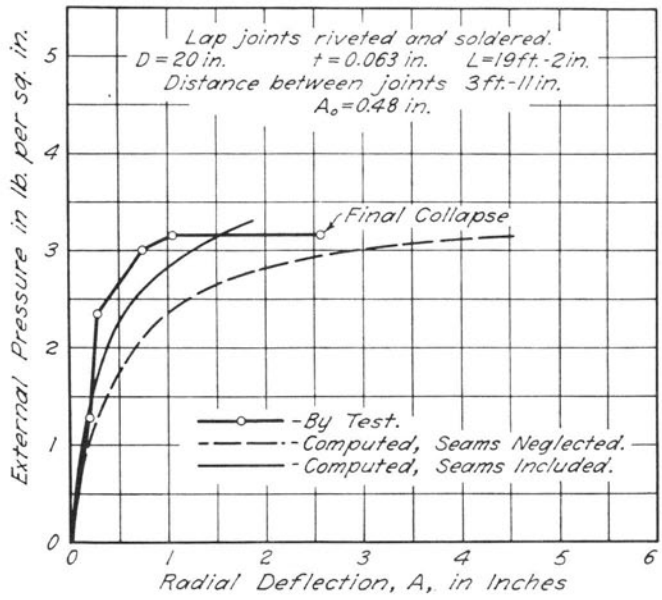

FIG. 17. RADIAL DEFLECTION CURVES—20-INCH STEEL PIPE WITH PRESSURE ON SIDES ONLY; $A_o = 0.48$ INCHES

For the 20-inch tube, with $\mu = 0.30$, and $N = 2$, $K_1 = 2.20$ and $K_2 = \dfrac{2}{3 \times 227^2}$. The collapsing pressure, with $E = 30{,}000{,}000$ lb. per sq. in., is $W_c = \left(K_1 + K_2 \dfrac{D^2}{t^2}\right) \dfrac{Et^3}{D^3} = (2.20 + 1.30)\ 0.94 = 3.29$ lb. per sq. in.

Maximum deflections were computed from

$$A = \frac{W}{W_c - W} A_o. \tag{57}$$

The moment of inertia of the shell and seams is approximately $I' = 0.006$ in.[4] The equivalent thickness is computed from $1/12Lt_s^3 = 0.006$ to be $t_s = 0.067$ in. The collapsing pressure then for $\dfrac{D}{t_s} = 298$ is $W_c = 3.82$ lb. per sq. in.

The deflection of the seam is practically the same as that of the shell. The seam adds little to the longitudinal stiffness of the shell.

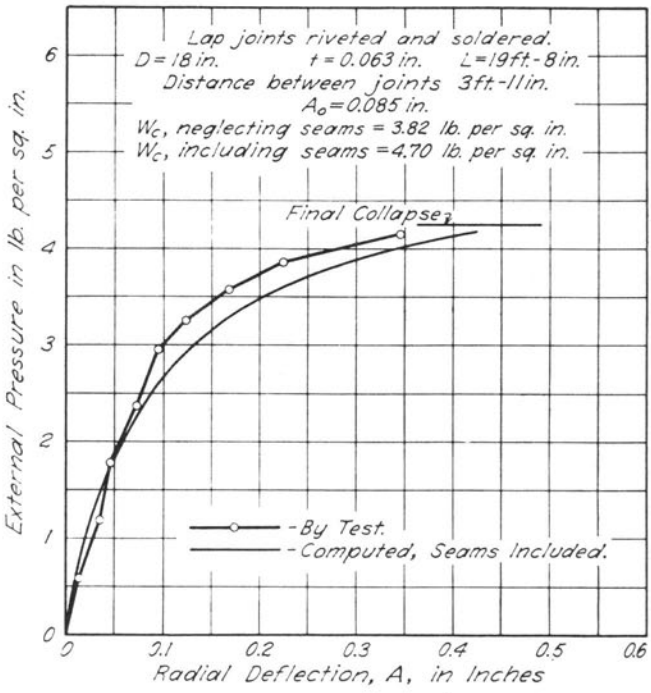

FIG. 18. RADIAL DEFLECTION CURVES—18-INCH STEEL PIPE WITH PRESSURE ON SIDES ONLY

However, it does add to the circumferential stiffness which is evident from the closer agreement between measured and computed deflections in which the stiffness of the combined shell and seams is taken into account. The computed collapsing pressure of the shell between seams, if the seams are strong enough, is several times as great as that of the shell as a whole using the increased stiffness of the shell and seams. No serious permanent set was indicated since the curve for decreasing pressure follows very closely the curve for increasing pressure.

The results of the second set of tests have been plotted in Figs. 17 and 18.

From Fig. 17 it may be noted that consideration of the seams as stiffeners gives closer agreement between measured and computed deflections. Figures 13 to 15 show views of the 20-in. iron pipe after collapse, and Fig. 19 shows a view of the 18-in. iron pipe after failure.

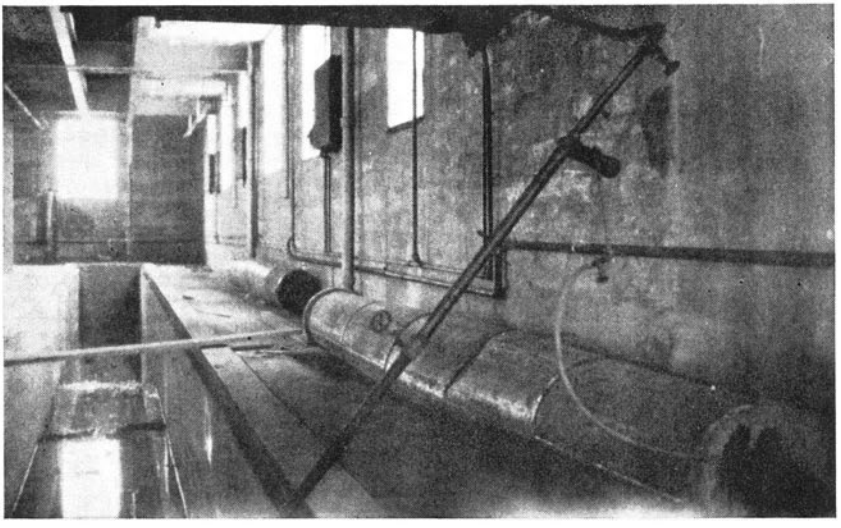

FIG. 19. VIEW OF 18-INCH STEEL PIPE AFTER COLLAPSE

B. Tests at the Research Laboratories of The Aluminum Company of America

24. *Object of Tests.*—The object of these tests was to determine experimentally the behavior and strength of cylinders having restrained edges. Specimens with various lengths and various D/t ratios were tested. In some tests external pressure was applied to the sides only, while in others, external pressure was applied to both the sides and ends. Initial "out-of-roundness" was considered and measured, but no attempt was made to obtain prescribed amounts of initial deviation from a round cylinder.

25. *Specimens and Materials.*—Tests were made on extruded aluminum alloy tubes and cylinders fabricated from aluminum alloy sheet.

The specimens were cut from

(1) A formed tube, 12 in. O.D., wall thickness 0.028 in.; D/t ratio about 430; cylinder formed from 3S-3/4H[33] sheets with edges butt-welded, longitudinal and circumferential seams hammered and dressed to about the same thickness as the sheet.

(2) Extruded seamless tubing, 6-in. O.D., wall thickness 0.061 in.; D/t ratio about 98.5; material 3S-H.

(3) Extruded seamless tubing 6-in. O.D.; wall thickness 0.042 in.; D/t ratio about 143; material 3S-H.

TABLE 1
TENSILE PROPERTIES OF THE ALUMINUM ALLOYS IN THE TUBES AND STIFFENERS*

Tube Size in.	Alloy	Proportional Limit lb. per sq. in.	Yield Strength lb. per sq. in.	Ultimate Strength lb. per sq. in.	Modulus of Elasticity¶ lb. per sq. in.
6.00 x 0.061	3S-H	10 000	25 000	28 000	10 000 000
6.00 x 0.042	3S-H	10 000	25 700	28 200	10 000 000
12.00 x 0.028	3S-3/4H	9 000	22 000	25 000	10 000 000
12.00 x 0.028	3S-O†	3 500‡	5 000	16 000	10 000 000

*Average values based on duplicate tests unless otherwise noted.
†Annealed portion of tube adjacent to welds.
‡Estimated value.
¶Modulus values determined to nearest 100 000 lb. per sq. in.

The average mechanical properties of the materials were determined from standard half-inch wide test coupons cut from the tubes after they were tested. These properties are given in Table 1. The measured diameters of the extruded tubes (as received) were within ± 0.008 in. of the nominal value at all sections, whereas most of them were within ± 0.005 in. The thickness varied between ± 5 per cent of the nominal value for these tubes. The diameters of the fabricated tube varied by as much as ± 0.127 in. for a given section, and the thickness was within ± 5 per cent of the nominal.

Where lateral pressure alone was applied, the ends of the tubes were sealed with aluminum plate bulkheads, discs one inch thick, fitted to the inside of the tubes. The bulkheads were separated by means of a 3-in. iron pipe which carried the end thrust. Each separator was held in a central position by centering discs and a rod. A rubber tube was pressed into a groove between the bulkhead and the tube to effect an airtight seal. The bulkheads were machined to fit the smallest of the tubes of the same nominal size. This procedure worked very well for the extruded tubes, but in some of the tubes formed from sheet clearances as great as 0.05 in. existed, and no fixity was obtained.

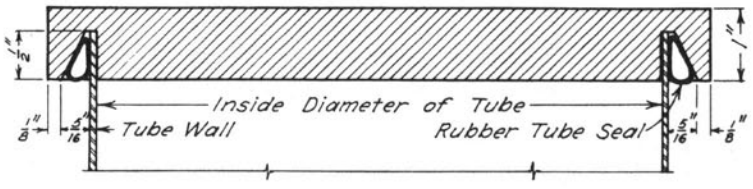

FIG. 20. SECTION THROUGH ALUMINUM-TUBE BULKHEAD

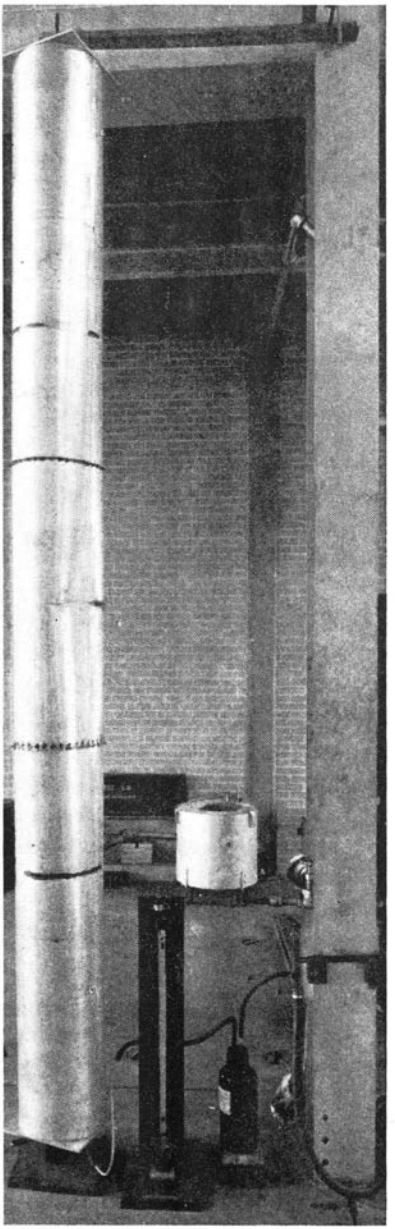

FIG. 21. ARRANGEMENT OF TEST EQUIPMENT AND SPECIMEN FOR TUBES REQUIRING PRESSURES LESS THAN 14 LB. PER SQ. IN. TO PRODUCE COLLAPSE

Where the pressure was applied to both the sides and ends of the tube, the bulkheads consisted of 1-in. thick aluminum plates somewhat larger in diameter than the tube to be tested (Fig. 20). Each bulkhead had a circular groove cut into it so that the tube would slide into the groove with a snug fit between the bulkhead and the inside of the tube. A space in the groove remained on the outside of the tube into which a rubber gasket was pressed to effect a seal. Clearances as great as 0.005 in. for the 6-in. tubes and 0.050 in. for the 12-in. tubes were encountered.

26. *Apparatus.*—For collapsing pressures less than 14 lb. per sq. in., external pressure was applied by producing a vacuum within the tube. An ordinary ejector vacuum pump was used to extract the air from the tubes. The differential pressure between the atmosphere and the interior of the tube was measured by means of a mercury manometer which was read to ± 0.05 in. of mercury. Figure 21 shows the arrangement of ejector pump, surge bottle, manometer, and tube for the test of a fabricated aluminum tube.

For collapsing pressures greater than 14 lb. per sq. in., external pressure was applied by placing the tube inside a drum filled with water and applying pressure by means of a hand hydraulic pump. The pressures were measured by means of a pressure gage reading to the nearest half pound. Figure 22 shows the test equipment.

Deflections were measured as changes in diameter by means of a dial caliper, shown in Fig. 23. Small V-shaped pieces of aluminum sheet were glued to the cylinder so that the points of the micrometer could be replaced at exactly the same point just inside of the V-notch. Separate calipers were made for the 6-in. and the 12-in. tubes. The dial gage was graduated to 0.001 in. of movement of the plunger, with which readings could be checked within ± 0.002 in.

27. *Procedure.*—For each test made with atmospheric pressure initial diameter readings were taken as follows: Six diameters 30 deg. apart on the 6-in. tubes and 12 diameters 15 deg. apart on the 12-in. tube. The diameters were measured at several sections along the tube for some of the long tubes, generally including a section at the center, one near a quarter point, and one near an end. For the short tubes (less than 3 diameters long) the diameters were measured at mid-length. On some of the tubes diameter readings were taken at several increments of pressure, the first being about one-fifth to one-third of the computed collapsing pressure, and the

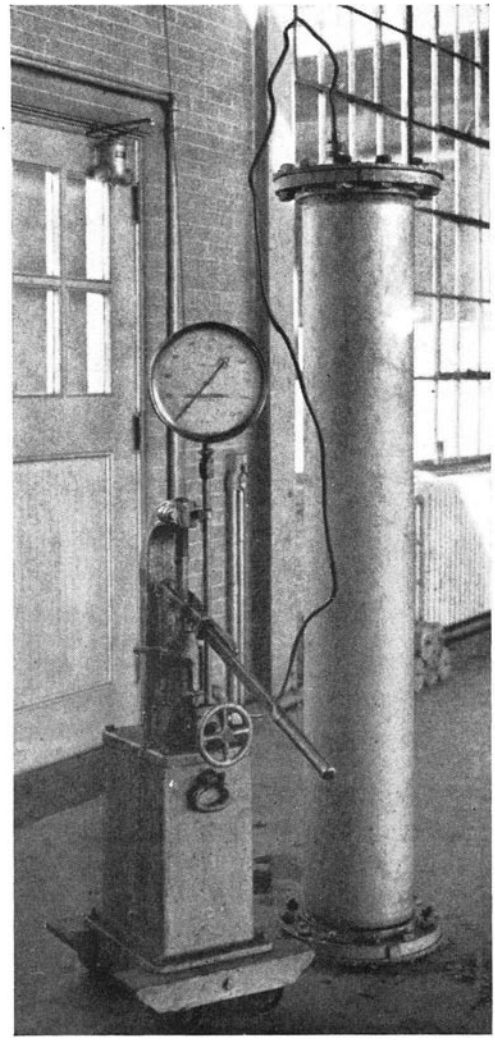

FIG. 22. ARRANGEMENT OF TEST EQUIPMENT AND SPECIMEN FOR TUBES REQUIRING PRESSURES GREATER THAN 14 LB. PER SQ. IN. TO PRODUCE COLLAPSE

others at about equal increments until either collapse impended or the deformations were so great that they were beyond the range of the calipers.

The long thin tubes which collapsed at stresses appreciably below the elastic limit tended to spring back to their initial shapes after the pressure was released. Those portions of the long tubes which

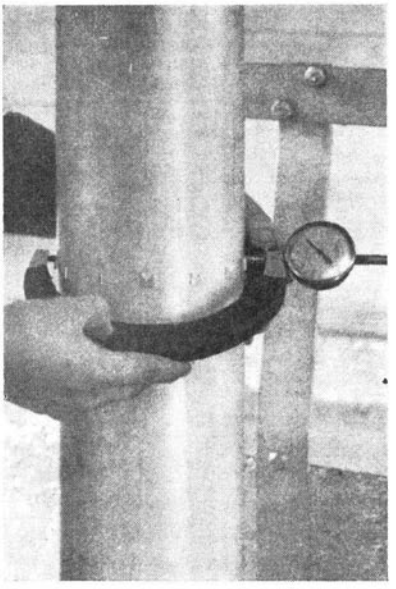

FIG. 23. METHOD OF MEASURING DIAMETER, 6-INCH O.D. TUBING

showed no appreciable permanent set were sawed off to be used as short specimens.

For specimens tested in the hydraulic pressure chamber, measurements for change of diameter were not made, and only the collapsing pressure and the number of lobes were determined.

28. *Results and Discussion.*—Tables 2 and 3 show a summary of the results of the tests on the aluminum tubes, with computed values of collapsing pressures corresponding to each limiting case of edge restraint.

Figures 24 to 28 inclusive show the short tubes after collapse.

The computed collapsing pressure of the actual "out-of-round" tubes was determined in accordance with Section 16. For the 12-in. tube the properties of the partially annealed metal adjacent to the welds were used because any local yielding would cause excessive deflections and collapse. The value of $\beta = 0.15$ was used for all cases.

For tubes which were not measurably out-of-round but were stressed beyond the elastic range, the collapsing pressures were computed by Equation (68). The values of W_c, the collapsing pressure for a round elastic tube, were obtained from Charts 4, 7, 8, or 9, according to the conditions considered.

TABLE 2

COLLAPSING PRESSURES OF THIN-WALLED ALUMINUM ALLOY CYLINDERS

External Pressure Applied to Sides Only

Specimen No.	Outside Diameter in.	Thickness t in.	D/t	Net Length in.	L/R	Initial Out-of-Roundness		Actual Collapsing Pressure lb. per sq. in.	Average Stress in Wall at Collapse lb. per sq. in.	Actual Number of Lobes at Collapse	Computed Number of Lobes at Collapse		Computed Collapsing Pressure for Perfect Elastic Cylinders lb. per sq. in.		Computed Collapsing Pressure for Aetual Tubes lb. per sq. in.	
						Maximum Radial Distortion in.‡	Number of Lobes				Edges Fixed	Edges Supported	Edges Fixed	Edges Supported	Edges Fixed	Edges Supported
2	11.90	0.028	425.0	23.0	3.86	0.016	4	3.68	780	4	6	5	5.72	3.64	4.70	3.05
3	11.90	0.028	425.0	16.5	2.77	0.007	2	5.16	1 100	5	7	6	7.41	5.33	6.50	4.70
4	11.90	0.028	425.0	13.5	2.27	(*)	(*)	5.90 ± ¶	1 250	5	8	7	9.10	6.63	....	....
5	11.92	0.028	425.0	10.5	1.77	0.006	3	8.80	1 870	7	9	8	11.45	8.45	9.40	7.20
1	11.92	0.028	425.0	143.0	24.0	0.025	2	0.715§	150	2	3	2	0.81	0.81	0.74	0.74
6	6.01	0.061	98.5	34.5	11.5	0.001	2	57	2 800	2–3**	3	2	70.0	49.2	69.2	48.7
7	6.01	0.061	98.5	22.5	7.5	(†)	(*)	87	4 400	3	3	3	107.8	74.3	107.8	74.3
8	6.01	0.061	98.5	10.5	3.5	(†)	(*)	170	8 400	4	5	3	241.0	163.0	226.0	163.0
9	6.01	0.061	98.5	7.5	2.5	(†)	(*)	290	14 300	5	5–6	4–5	345.0	240.0	275.0	225.0
10	6.00	0.042	143.0	43.5	14.5	0.013	2	16.5	1 180	2	3	2	22.6	13.5	21.4	12.5
11	6.00	0.042	143.0	32.0	10.7	(†)	(*)	24.0	1 710	3	3	2–3	28.7	22.2	28.7	22.0
12	6.00	0.042	143.0	21.0	7.0	(†)	(*)	31	2 220	3	4	3	46.6	29.3	46.6	29.3
13	6.00	0.042	143.0	15.75	5.25	(†)	(*)	40	2 860	4	4	3–4	61.6	43.8	61.6	43.8
14	6.00	0.042	143.0	10.75	3.58	(†)	(*)	63	4 500	(*)	5	4	92.0	64.0	92.0	64.0
15	6.00	0.042	143.0	7.00	2.33	0.001	(*)	100	7 150	5	6	5	147.0	102.0	138.0	96.0
16	6.00	0.042	143.0	5.00	1.67	(†)	(*)	165	11 800	6	7	6	205.0	154.0	175.0	146.0

*Not measured.
†Less than 0.001 in.
‡Determined from diameter measurements.
¶Collapsed unexpectedly on preliminary test of equipment. Ends slipped on bulkhead.
§Tube stiffened at approximately the third points by single angle rings (0.125 x 0.25 x 0.042) short leg outstanding. Outstanding flange buckled. Stiffened shell independent of end conditions.
**Where two numbers appear the lobes in the tested tube were not distinct and might have been either number.
$\mu = 0.30$.

TABLE 3

COLLAPSING PRESSURES OF THIN-WALLED ALUMINUM ALLOY CYLINDERS

External Pressure Applied to Sides and Ends

Specimen No.	Outside Diameter $D=2R$ in.	Thickness t in.	D/t	Net Length L in.	L/R	Initial Out-of-Roundness		Actual Collapsing Pressure lb. per sq. in.	Average Stress in Wall at Collapse lb. per sq. in.	Actual Number of Lobes at Collapse	Computed Number of Lobes at Collapse		Computed Collapsing Pressure for Perfect Elastic Cylinders lb. per sq. in.		Computed Collapsing Pressure for Actual Tubes lb. per sq. in.	
						Maximum Radial Distortion in.‡	Number of Lobes				Edges Fixed	Edges Supported	Edges Fixed	Edges Supported	Edges Fixed	Edges Supported
17	11.90	0.028	425.0	143.0	24.0	0.092	2	0.563	120	2	3	2	0.83	0.57	0.72	0.50
18	11.90	0.028	425.0	48.0	8.0	0.048	2	1.033¶	220	2¶	....	3	....	1.64‡‡	....	1.20
												2	....	1.41††	....	1.00
19	11.90	0.028	425.0	143.0	24.0	0.127	2	0.585§	125	2	....	2	....	0.81	....	0.57
20	11.90	0.028	425.0	23.0	3.86	0.025	3	3.20	680	4	6	5	4.95	3.66	3.90	2.90
21	11.90	0.028	425.0	14.0	2.35	0.010	(*)	5.55	1 180	5	8	6–7**	8.10	6.00	6.70	5.10
22	11.90	0.028	425.0	11.0	1.85	0.006	(*)	7.36	1 560	7	9	7	10.70	7.30	8.80	6.10
23	6.01	0.061	98.5	59.25	19.75	(†)	(*)	29.0	1 430	2	2	2	35.8	26.3	35.8	26.3
24	6.01	0.061	98.5	34.2	11.4	(†)	(*)	53.0	2 610	2–3**	3	2	71.5	45.2	71.5	45.2
25	6.01	0.061	98.5	23.2	7.7	(†)	(*)	81.0	4 000	3	3	3	95.0	62.0	95.0	62.0
26	6.01	0.061	98.5	11.2	3.7	0.002	2	155.0	7 640	3–4**	4–5**	3	226.0	152.0	180.0	110.0
27	6.01	0.061	98.5	8.25	2.75	(†)	(*)	240.0	11 800	4–5**	5	4	321.0	216.0	264.0¶¶	211.0¶¶
28	6.01	0.061	98.5	5.25	1.75	(†)	(*)	330.0	16 300	6	6–7**	6	505.0	358.0	326.0¶¶	274.0¶¶
29	6.01	0.061	98.5	5.25	1.75	(†)	(*)	330.0	16 300	6	6–7**	6	505.0	358.0	326.0¶¶	274.0¶¶
30	6.01	0.042	143.0	19.0	6.3	(†)	(*)	34.0	2 400	3	4	3	51.7	34.2	151.7	34.2
31	6.01	0.042	143.0	14.0	4.7	0.006	3	45.0	3 200	3	4	3–4**	66.8	46.2	60.0	40.0
32	6.01	0.042	143.0	11.0	3.7	0.008	3	55.0	3 900	4–5**	5	4	92.5	58.2	72.0	49.0
33	6.01	0.042	143.0	8.5	2.8	0.003	4	75.0	5 350	Irregular	6	5	120.0	82.2	00.0	70.5

*Not measured.

†Less than 0.001 in.

‡Determined from diameter measurements.

¶Tube stiffened at approximately third points by angle rings (0.30 x 0.25 x 0.042); long leg outstanding. Tube distorted somewhat between stiffeners, then outstanding flange of stiffener buckled.

§Tube stiffened at approximately third points by angle rings (0.125 x 0.25 x 0.042); short leg outstanding.

**Where two numbers appear the lobes in the tested tube were not distinct and might have been either number.

††Based on strength of ring.

‡‡Based on strength of short section of tube between rings.

¶¶Stresses above the elastic limit of the material, values computed using E'.

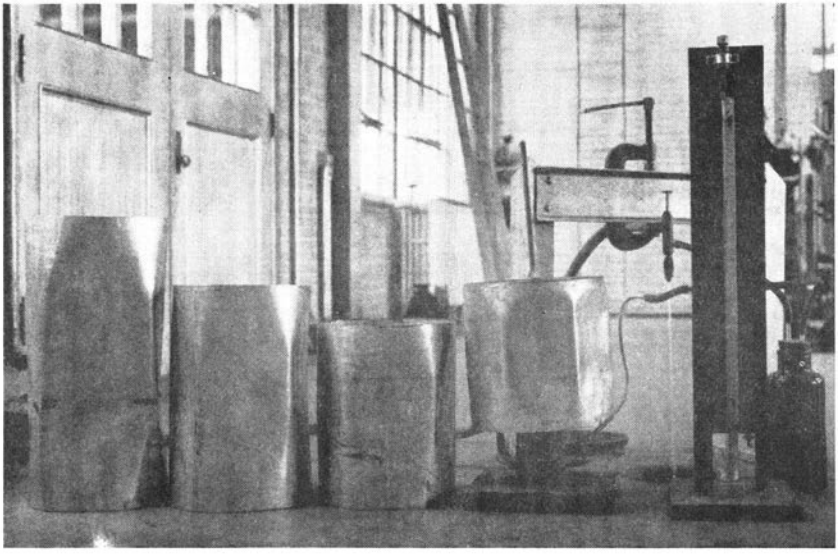

FIG. 24. SPECIMENS 2, 3, 4, AND 5 AFTER TEST, AND LOW PRESSURE APPARATUS

Deflection measurements were made on Specimens No. 17, No. 18, No. 1, No. 10a, and No. 10b. The results of these tests are discussed individually in the order in which they were obtained.

Specimen No. 17. This specimen was a 12-in. diameter tube formed from 21-gage (0.028 in. thick) sheet. The circumferential seams were about 36 in. apart, giving a total length of about 144 in. for four sections. The net length (clear distance between bulkheads) was 143 in. Pressure was applied to both the sides and the ends, i.e., the end thrust from the bulkheads was carried by the specimen. Figure 29 shows the plotted values of deflection together with the maximum stresses. Apparently the edges were about half-way between fixed and simply supported. The deflection was so gradual that the tube could be made to breathe in and out, reproducing the same deflection at given pressures whether the load was increasing or decreasing. This specimen was used for demonstration for some time, and was deflected (A = about 0.30 in.) probably fifty times.

Specimen No. 18. This specimen was the former Specimen No. 17 stiffened with two single angle (0.30 x 0.25 x 0.043 in.) stiffening rings, one on each side at 18 in. from the center of the tube. The rings were made from 3S-3/4H material, and were attached to the shell with No. 2 machine screws spaced 1 in. center to center. These

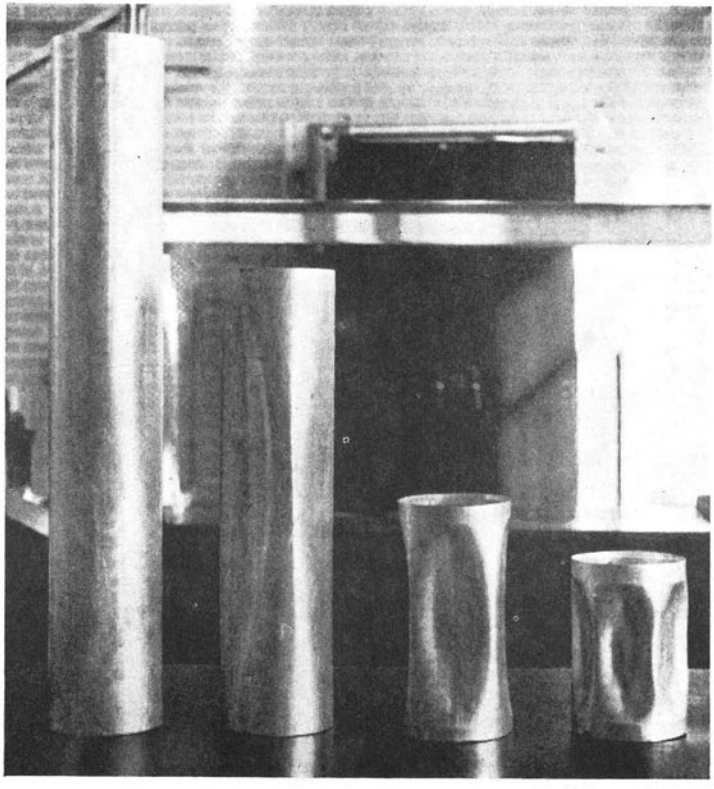

FIG. 25. SPECIMENS 6, 7, 8, AND 9 AFTER TEST

rings were intended to give about the smallest size of stiffener which would develop the intermediate shell. Specimen No. 18 was tested under the same conditions as Specimen No. 17.

Figure 30 shows the deflection and stress. Note the agreement between measured and computed values of radial deflection of the stiffeners. The deflections shown are the average values for the two stiffeners, each of which did not deviate more than 0.005 in. from the average. Until collapse, the deflection of the shell midway between the stiffeners was about 20 per cent greater than the corresponding deflection at the stiffener. Figure 21 shows the specimen after failure. The lower stiffener buckled and the lower end-section collapsed before the center section collapsed. No measurements of diameter of the lower end section were obtained for this test. Since failure occurred by buckling of the outstanding flange of the stiffener there is no decisive evidence that the moment of inertia of the com-

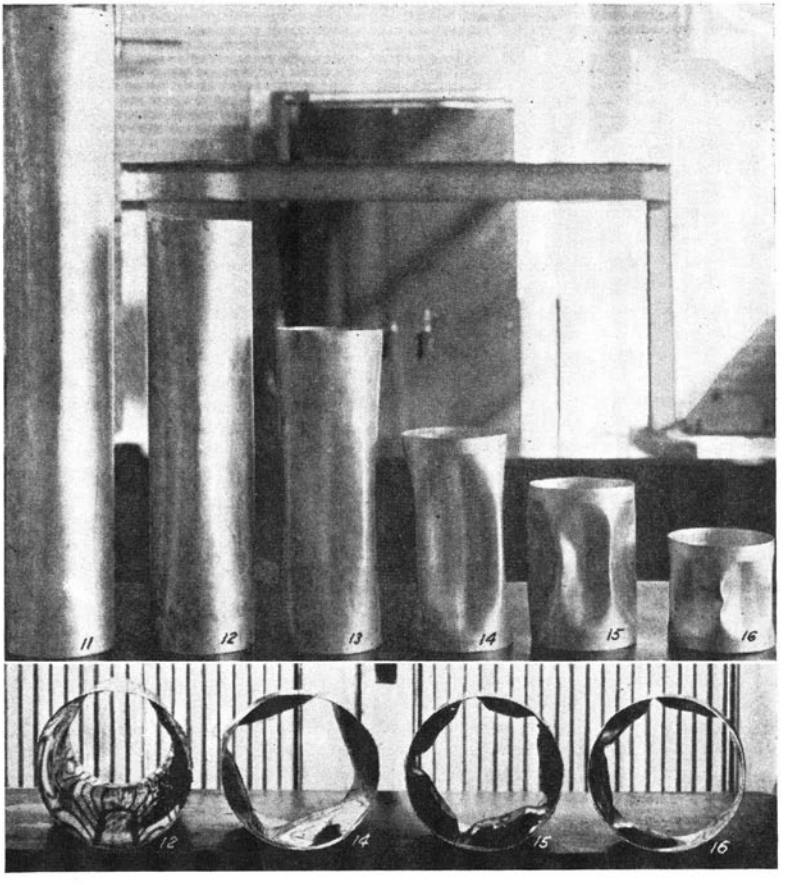

FIG. 26. SPECIMENS 11, 12, 13, 14, 15, AND 16 AFTER TEST

bined stiffener and plate was adequate to develop the strength of the short lengths of the tube between stiffeners or between stiffener and bulkheads.

Specimen No. 1. After Specimen No. 18 was tested the tube was brought back to a "nearly round" condition by hammering from the inside and by straightening the outstanding leg of the stiffener. The outstanding leg of the stiffener was then cut down to a height of $\frac{1}{8}$ in. to make Specimen No. 1. The same measurements were made on this specimen as on Specimen No. 18. Pressure was applied to the sides only, the end thrust being carried by an iron pipe inside the specimen, as previously described.

Deflection and stress curves are shown in Fig. 31. The computed

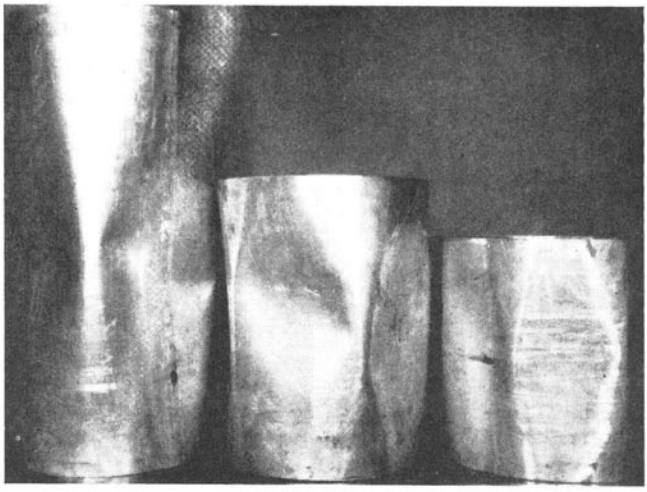

FIG. 27. SPECIMENS 20, 21, AND 22 AFTER TEST

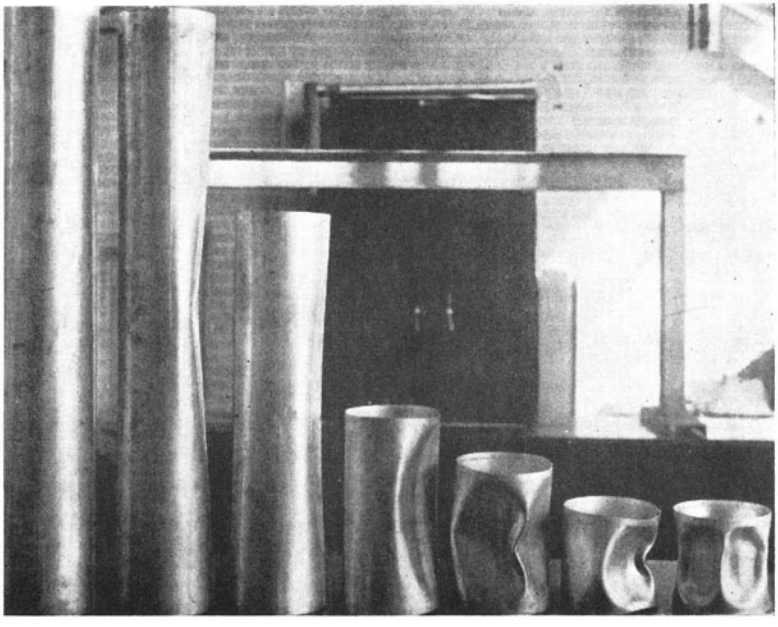

FIG. 28. SPECIMENS 23, 24, 25, 26, 27, 28, AND 29 AFTER TEST

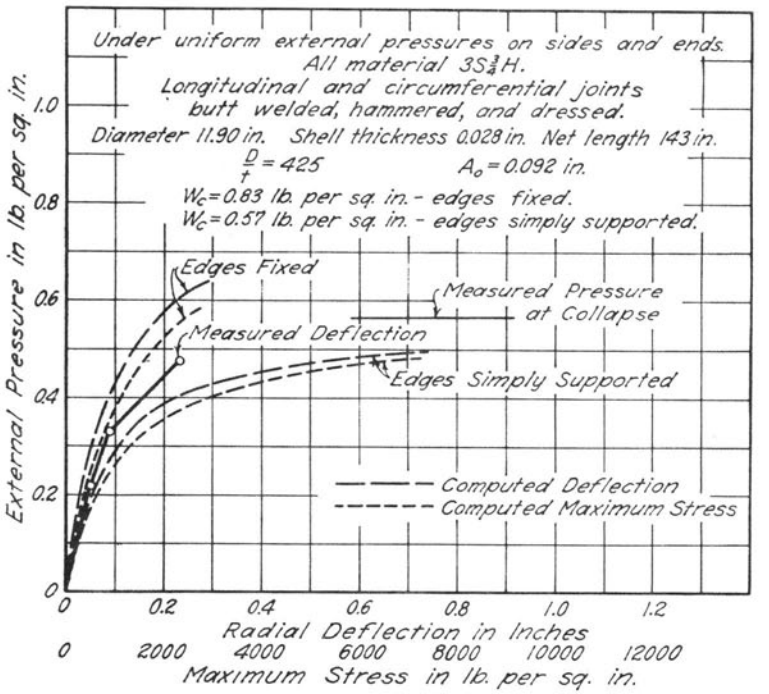

FIG. 29. RADIAL DEFLECTION AND MAXIMUM STRESS CURVES, SPECIMEN NO. 17, WELDED ALUMINUM ALLOY TUBE

collapsing pressure (Table 2) is determined as follows: assuming failure as collapse of a short tube between stiffeners simply supported at the stiffeners,

$$\frac{L}{R} = \frac{36}{5.96} = 6.05, \quad \frac{D}{t} = \frac{11.92}{.028} = 425, \quad K \text{ (from Fig. 4)} = 17,$$

$$W_c = KE\left(\frac{t}{D}\right)^3 = 17 \times 10^7 \times \frac{1}{(425)^3} = 2.20 \text{ lb. per sq. in.}$$

Between the stiffener and the end the clear length is 53.5 in. For this section one edge is fixed and the other simply supported.

The equivalent thickness t_s for the member, considered as a long tube, is computed from $I_s = \frac{1}{12} b t_s^3$ in which $b = 36$ in. and I_s, the total moment of inertia, is 0.000098 in.[4] For this computation a

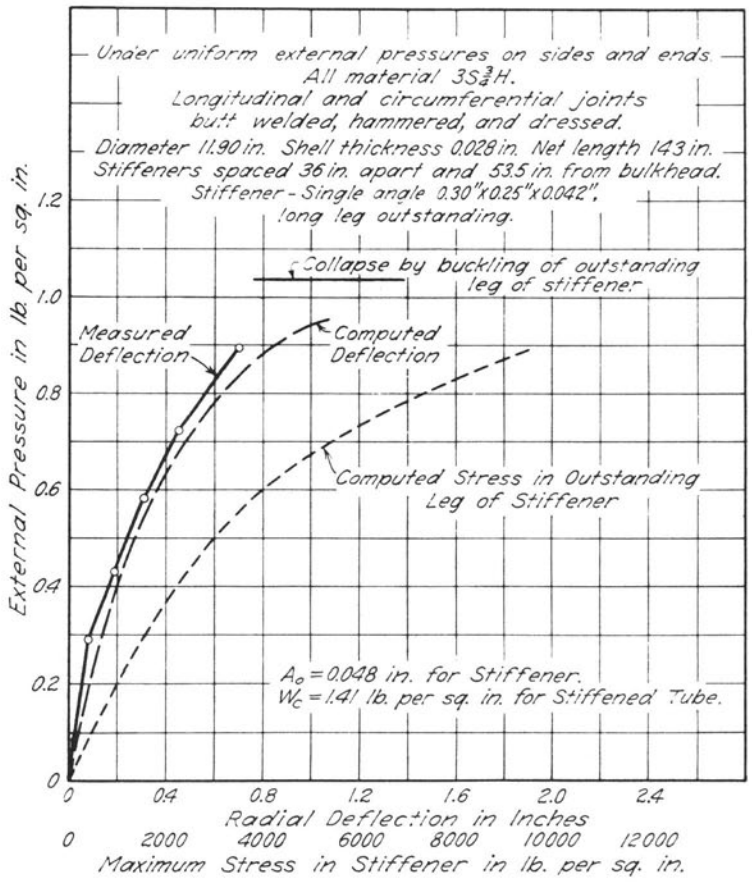

FIG. 30. RADIAL DEFLECTION AND MAXIMUM STRESS CURVES, SPECIMEN NO. 18, WELDED ALUMINUM ALLOY TUBE

length of $30t$ is assumed as acting with the stiffening angle. Then $t_s = 0.032$ in., $D/t_s = 372$, $L/R = 24$, $K = 4.2$, and $W_c = 0.815$ lb. per sq. in. Since this value is less than 2.20, the tube is expected to fail as a whole.

Stress in the stiffener flange is computed from Equation (63). The maximum moment is

$$M_s = EI_s \frac{3A_o}{R_s^2} \frac{W}{W_c - W}.$$

The bending stress is $M_s c_s / I_s$. The average bending stress in the stiffener is computed by using $c_s = 0.057$ in., the distance from

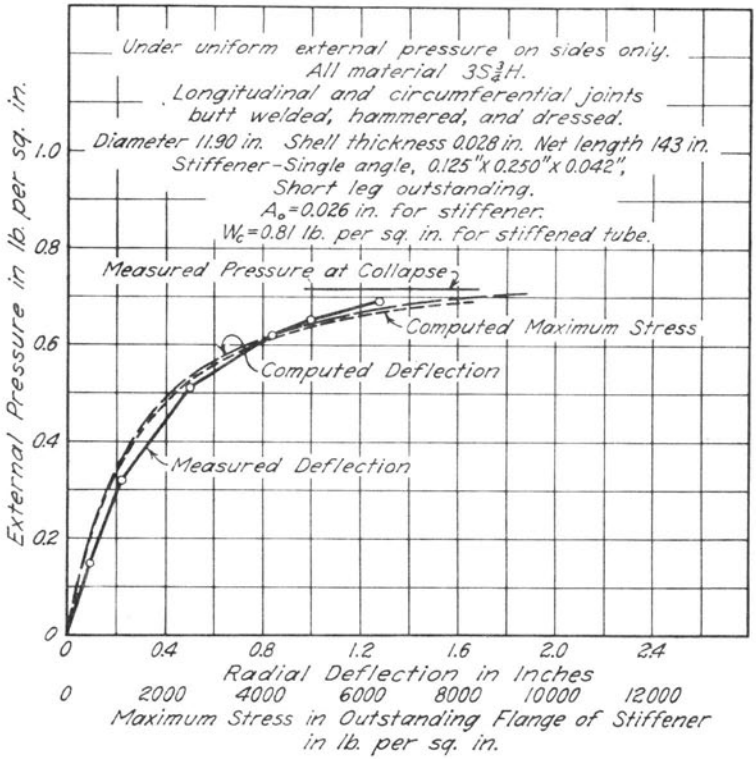

FIG. 31. RADIAL DEFLECTION AND MAXIMUM STRESS CURVES, SPECIMEN NO. 1, WELDED ALUMINUM ALLOY TUBE

the neutral axis of the stiffener section (angle and plate) to the midpoint of the outstanding flange. With $A_o = 0.026$ and $R_s = 5.98$, the average stress is $S = 1250 \dfrac{W}{W_c - W}$.

For $W = 0.715$, $S = 8\,950$ lb. per sq. in.

For $W = 0.74$, $S = 12\,300$ lb. per sq. in.

This stress is above the proportional limit, hence the resistance is reduced. By Equation (67)

$$\frac{E'}{E} = 1 - \frac{1}{4}\left(\frac{12\,300 - 9000}{25\,000 - 1000}\right)^2 = 0.995.$$

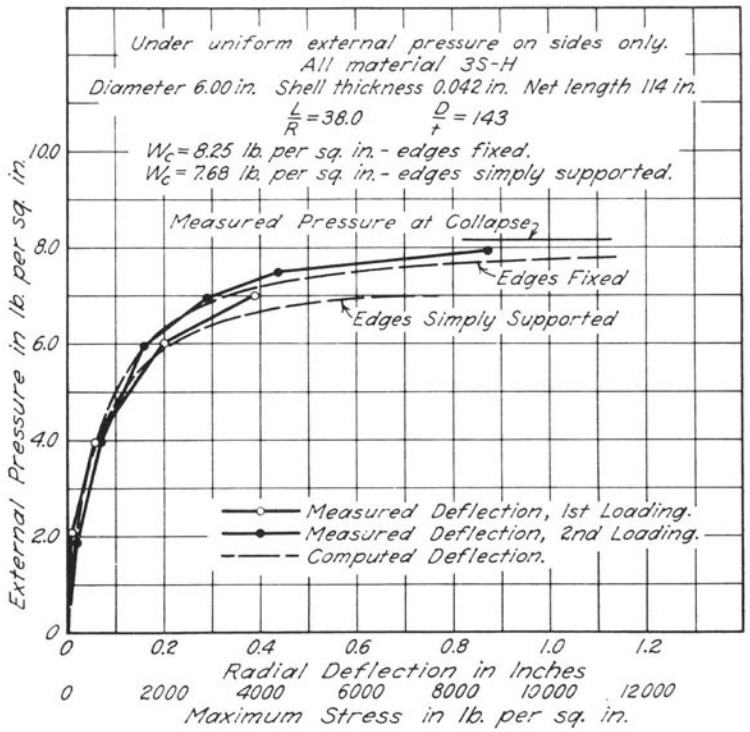

FIG. 32. RADIAL DEFLECTION AND MAXIMUM STRESS CURVES, SPECIMEN NO. 10a, EXTRUDED ALUMINUM ALLOY TUBE

The corrected W_c is $0.995 \times 0.815 = 0.810$ lb. per sq. in.

Then $$s = 1250 \times \frac{0.74}{0.07} = 13\ 200 \text{ lb. per sq. in.}$$

with a corrected value for $E'/E = 0.993$.

Hence W_c is very nearly 0.74 lb. per sq. in.

Specimen No. 10a. Specimen No. 10a was one of the 6 in. x 0.042 in. extruded tubes, 10 ft. long over-all. The pressure was applied on the sides only, while the end thrust was carried by an inner iron pipe which was 9 ft.-6 in. long, the effective length of the specimen thus becoming 9 ft.-6 in. External pressure was applied gradually until the deflections started increasing rapidly. The pressure was then released and later a demonstration test (second test) was made

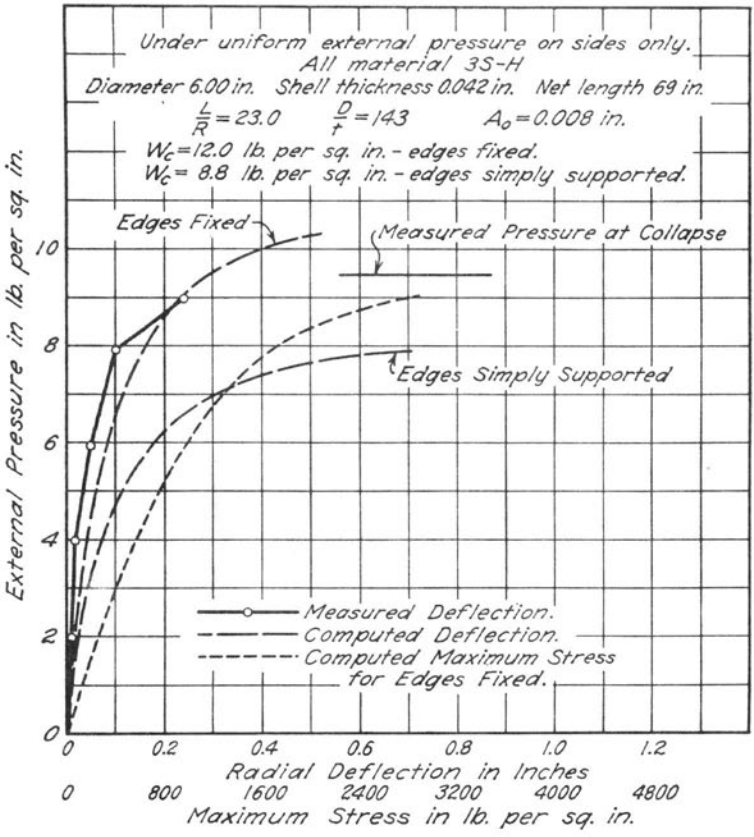

FIG. 33. RADIAL DEFLECTION AND MAXIMUM STRESS CURVES, SPECIMEN NO. 10b, EXTRUDED ALUMINUM ALLOY TUBE

in which the loading was continued until collapse occurred. After the first test the central section of the tube retained a slight permanent set, not more than 0.010 in., which was practically removed by pressing this part of the tube by hand into an elliptical shape so as to oppose the permanent set. The data are plotted in Fig. 32.

The bulkheads for sealing the ends of this specimen were made and fitted for it. Therefore the edges at the ends of this tube would be expected to be nearly fixed. The values computed for the condition of fixed edges agree with the test data much more closely than do the values based on simply supported edges. The computed collapsing pressure for fixed edges is 0.805 lb. per sq. in., which is close to the actual pressure, (0.811 lb. per sq. in.).

Specimen No. 10b. This specimen was 6 ft. long, cut from one end of Specimen No. 10a, and was tested without end pressure. The inner pipe was 5 ft.-9 in. long, making that the effective length. One end of this specimen fitted the bulkhead snugly, but the other did not, consequently the fixation of the edges was not complete. Nevertheless, the tube, which was slightly out-of-round, carried more than the computed value for a perfect tube with edges simply supported.

The test data are plotted in Fig. 33 together with computed values. The values of deflection are appreciably smaller than the computed values based on the measured 0.008 in. initial radial deviations from a round cylinder with fixed edges. Since the initial out-of-roundness was small, reasonable errors in measuring this value would be more than enough to account for the discrepancy. At a pressure of about 8.9 lb. per sq. in., the measured deflections show a rapid increase which indicates a value of W_c less than that for fixed edges.

VIII. Summary and Conclusions

29. *Summary of Analytical Results.*—The collapsing pressure per unit of area, W_c, for thin-walled round cylinders under a uniform external pressure is equal to the product of the collapsing stiffness, KE, and the cube of the t/D ratio (thickness to diameter) of the cylinder:

$$W_c = KE\,(t/D)^3$$

E for linear elastic action (Hooke's law) is the modulus of elasticity of the material in the shell, and for non-linear or plastic behavior a modified modulus denoted by E' is used.

Curves showing values of K for varying t/D and L/R (length to radius) ratios under several load and edge conditions are given in the figures listed:

Load	Edges at Ends	Figure
Uniform pressure on sides only	Simply supported	4
Uniform pressure on sides only	Fixed	6
Uniform pressure on sides and ends	Simply supported	8
Uniform pressure on sides and ends	Fixed	9

Axial End Load.—For linear elastic behavior the collapsing force P_c per unit of length of circumference, for a round cylinder under an axial load distributed uniformly around the circumference, is given

by Equation (47). For small values of t/R (thickness to radius) and Poisson's ratio $\mu = 0.30$ Equation (47) reduces to

$$S_c = 0.6E\frac{t}{R} \tag{49}$$

where $S_c = \dfrac{P_c}{t}$ is the stress per unit area in the shell at the collapsing load.

Stiffened Cylinders.—For round cylinders stiffened with rings, the collapsing pressure is computed from $W_c = KE(t/D)^3$ for a length of cylinder L_s, between the rings, provided the rings are sufficiently strong and stiff so that they do not fail. The flexural stiffness, EI_s, of the stiffener which is necessary to withstand a pressure W_s is given by Equation (53),

$$EI_s = \frac{W_s D^3 L_s}{24}.$$

I_s is the moment of inertia of the ring section and that part of the shell which has been assumed to act with the ring.

Cylinders "Out-of-Round".—The radial deflection of a cylinder slightly out-of-round proceeds gradually to the final failure. Under a uniform external pressure, W, the deflection A is expressed by Equation (55),

$$A = \frac{WA_o}{W_c - W}.$$

A_o is the maximum initial deviation of the out-of-round cylinder from a round one. The initial radial deviations are of the same general pattern as the finally deflected shell.

The maximum circumferential stress in the shell is given by Equation (57), and the maximum pressure that causes a given stress is expressed by Equation (61).

Non-linear or Plastic Action.—If the action is non-linear or plastic, a modified modulus of elasticity E' is proposed for use in the collapsing formula for W_c. Two cases are of note: (1) when the average stress in the shell or stiffener is less than the proportional

limit Q^* of the material the modulus is reduced according to Equation (67) page 43.

$$E' = E\left[1 - \frac{1}{4}\left(\frac{S - Q}{S_u - S_1}\right)^2\right]$$

in which S is the maximum stress (direct and bending) in the shell, S_u is the modulus of rupture of the material, and S_1 is the average stress in the shell; (2) when the average stress is greater than the proportional limit, E' is estimated to be equal to the tangent modulus at a stress equal to the average stress. The use of the modified modulus is illustrated in the computations for the collapsing pressure of an actual tube, specimen No. 1, on page 62.

For combined external pressure and longitudinal stress the effect of biaxial stress upon the inception and nature of plastic action must be considered. The stress causing a start of plastic action under combined stress may be computed from Equation (69),

$$S_1^2 - S_1 S_p + S_p^2 = S_y^2.$$

30. *Comparison of Analytical With Experimental Behavior of Aluminum Tubes.*—The values compared are the following ratios obtained from Tables 2 and 3.

S = average collapsing pressure by analysis, simply supported edges.

F = average collapsing pressure by analysis, fixed edges.

T = average collapsing pressure by test.

Load	Roundness	Number of Values Averaged	T/S	F/T	F/S
Sides only	Round and out-of-round	15	1.05	1.33	1.40
	Round	5	1.04	1.36	1.43
	Out-of-round	10	1.16	1.17	1.36
Sides and Ends	Round and out-of-round	14	1.02	1.44	1.47
	Round	4	1.14	1.31	1.50
	Out-of-round	10	1.16	1.20	1.40

No tests of shells with end pressure only were made as a part of this investigation. Tests reported in Bulletins 255 and 292 of the Engineering Experiment Station of the University of Illinois resulted in a wrinkling stress considerably smaller than S_c given by Equation (49).

*See Section 6, Notation.

31. *Conclusions.*—From the analytical results, the test data, and a comparison thereof, the following conclusions are drawn:

A. Effect of Edge Restraint

(1) A fixed-edge condition as expressed analytically has a marked effect on the collapsing pressure of a round thin-walled cylinder with an L/R ratio between 1 and 80 and a D/t ratio between 20 and 1000, for uniform side pressure only or uniform side and end pressure.

For a given collapsing pressure the maximum effect is equivalent to increasing the L/R ratio by 40 to 50 per cent.

(2) Analytical values of the collapsing pressure for both round and out-of-round cylinders with edges simply supported are on the average less than the values obtained by test for both types of load, uniform side pressure only, and uniform side and end pressure.

(3) The analytical values of the collapsing pressure for both round and out-of-round cylinders with fixed edges are considerably higher on the average than the test values obtained with both types of load.

(4) Test results indicate that some degree of restraint existed in most of the tests but the degree of restraint could not be definitely determined.

B. Effect of Out-of-Roundness

(5) Analytically the effect of out-of-roundness varies with the ratio of initial radial deflection A_o to the thickness t of the shell, the L/R (length-radius) ratio, the t/D (thickness-diameter) ratio, the elastic limit of the material, and the bending modulus of failure of the material. An expression of the effect is obtained for an initial out-of-roundness of the same pattern as the deflected shell at buckling.

C. Effect of Ring Stiffeners

(7) Analytically the collapsing pressure of thin-walled cylinders stiffened with circumferential rings may be computed as the collapsing pressure of the short lengths of cylinder between the stiffening rings, provided the stiffeners have sufficient strength and stiffness. A rigorous determination demands that uncertainties as to bending stiffness in the stiffened shell and as to kind of stress distribution in the stiffeners be removed. Tests on tubes with stiffeners are too few in number to draw definite conclusions.

D. Effect of Inelastic Action

(8) The expressions for the collapsing pressure may be applied to shells stressed beyond the elastic limit of the material if a modified "effective" modulus of elasticity is used.

The use of an empirical formula such as Equation (67) based upon the behavior of straight members under compressive loads for taking account of inelastic action in the curved shell needs further justification but may serve for design purposes until a more satisfactory method is developed.

E. Final

(9) The results obtained point to the need for the study of rather sharply curved members under buckling loads when the maximum stress in the member exceeds the elastic limit of the material; for further study on the effect of stiffeners on the collapsing pressure of tubes; for tests on tubes with measured restraints as to displacements and rotations at the ends; for further analytical and experimental investigation of the out-of-round tubes; and for tests on tubes subjected to combined external pressure and axial loads, particularly tensile loads.

This page is intentionally blank.

No.	Year	Author	Title and Reference
1	1848	William Fairbairn	"The Resistance of Tubes to Collapse," Philosophical Trans., Vol. 148, pp. 389-413.
2	June 1906	A. P. Carman and M. L. Carr	"The Resistance of Tubes to Collapse," Bull. No. 5, Eng. Exp. Sta., Univ. of Ill.
3	1917	A. P. Carman	"The Collapse of Short Thin Tubes," Bull. No. 99, Eng. Exp. Sta., Univ. of Ill.
4	1906	R. T. Stewart	"Collapsing Pressure of Bessemer Steel Lap-Welded Tubes, Three to Ten Inches in Diameter," Trans. A.S.M.E., Vol. 27, pp. 730-822.
5	Sept.-Dec. 1931	T. McLean Jasper and John W. W. Sullivan	"The Collapsing Strength of Steel Tubes," Trans. A.S.M.E., Vol. 53, APM-53-17b, pp. 219-245.
6	Sept.-Dec. 1931	H. E. Saunders and D. F. Windenburg	"Strength of Thin Cylindrical Shells Under External Pressure," Trans. A.S.M.E., Vol. 53, APM-53-17a, pp. 207-218.
7	Nov. 1934	D. F. Windenburg and C. Trilling	"Collapse by Instability of Thin Cylindrical Shells Under External Pressure," Trans. A.S.M.E., Vol. 56, APM-56-20, pp. 819-825.
8	1932	E. E. Lundquist	"Strength Tests of Thin-Walled Duralumin Cylinders in Compression," Tech. Memo. No. 427, of the Natl. Advis. Com. Aero.
9	1933	E. E. Lundquist	"Strength Tests of Thin-Walled Duralumin Cylinders in Compression," Report No. 473, of the Natl. Advis. Com. Aero.
10	Feb. 28, 1933	W. M. Wilson and N. M. Newmark	"The Strength of Thin Cylindrical Shells as Columns," Bull. No. 255, Eng. Exp. Sta., Univ. of Ill.
11	Nov. 1934	L. H. Donnell	"A New Theory for the Buckling of Thin Cylinders Under Axial Compression and Bending," Trans. A.S.M.E., Vol. 56, AER-56-12, pp. 795-806.
12	1888	G. H. Bryan	"Application of the Energy Test to the Collapse of Long Thin Pipe Under External Pressure," Proc. Cambridge Phil. Soc., Vol. VI, pp. 287-292.
13	1913	R. V. Southwell	"On the General Theory of Elastic Stability," Phil. Trans. Royal Soc. (London), Vol. 213, Series A, pp. 187-244.
14	May 1913 Sept. 1913 Jan. 1915	R. V. Southwell	"Collapse of Tubes," Phil. Mag., pp. 687-698; pp. 502-511; pp. 67-77.

No.	Year	Author	Title and Reference
15	July 1914	Gilbert Cook	"The Collapse of Short Thin Tubes by External Pressure," Phil. Mag., pp. 51-56.
16	1914	R. von Mises	"Der kritische Aussendruck zylindrischer Rohre," Vol. 58, pp. 750-755, V. D. I. Zeitschr.
17	1929 Aug. 1933	R. von Mises D. F. Windenburg	"Der kritische Aussendruck für allseits belastete zylindrische Rohre," A Stodola-Festschrift. Translated and annotated by D. F. Windenburg, Report No. 366 of the U. S. Exp. Model Basin, Navy Yard, Washington, D. C.
18	1920	K. von Sanden and K. Günther	"Ueber das Festigkeitsproblem querversteifter Hohlzylinder unter allseitig gleichmässigem Aussendruck," Werft Und Reederei, Vol. 1, No. 8, pp. 163-168; Vol. 1, No. 9, pp. 189-198; Vol. 1, No. 10, pp. 216-221.
19	1929 1931	T. Tokugawa	"Model Experiments on the Elastic Stability of Closed and Cross-Stiffened Circular Cylinders under Uniform External Pressure," Proc. World Eng. Congress, Tokyo, 1929, Vol. XXIX (1931), pp. 219-279.
20	1922	H. M. Westergaard	"Buckling of Elastic Structures," Trans. A.S.C.E., Vol. 85, pp. 576-654.
21	May 1928	H. M. Westergaard	"Report on Arch Dam Investigation," Part 3, Proc. A.S.C.E., pp. 231-266.
22	July 1933	H. M. Westergaard	"Stress Functions for Shells," Tech. Memo. No. 351, U. S. Bur. Recl.
23		A. Föppl and L. Föppl	"Drang und Zwang," Vol. 1, Second Ed., page 53, Eq. 59.
24	April 1935	E. E. Lundquist	"Strength Tests of Thin-Walled Duralumin Cylinders in Combined Transverse Shear and Bending," Natl. Advis. Com. Aero., Tech. Note No. 523.
25	May 1935	E. E. Lundquist	"Strength Tests of Thin-Walled Duralumin Cylinders of Elliptic Section," Natl. Advis. Com. Aero., Tech. Note No. 527.
26	1924	T. Claxton Fidler	"A Practical Treatise on Bridge Construction," Fifth Ed., page 162.
27	1889 1895 1890	F. Engesser	Zeitschr. Architektur und Ingenieurwesen. (Architekten-und Ingenieur-verein, Hannover.) Vol. 35, p. 455, Schweiz. Bauzeitung, Vol. 26, page 24; p. 731, V. D. I. Zeitschr., Vol. 34.
28	1891	A. Considère	"Résistance des Pièces comprimées Congres International des Procédés de Construction, Annexe a Comptes Rendus," page 382.

No.	Year	Author	Title and Reference
29	1910	Theodor von Kàrmàn	"Untersuchungen über Knickfestigkeit," Mitteilungen über Forschungsarbeiten auf dem Gebiete des Ingenieurwesens, 81, Berlin.
30	March 1935	William R. Osgood	"The Double-Modulus Theory of Column Action," Civil Engr. Vol. 5, No. 3, page 173.
31	1928	H. M. Westergaard and W. R. Osgood	"Strength of Steel Columns," Trans. A.S.M.E., Vol. 50, Part I, paper No. APM-50-9, p. 65.
32	1929	L. B. Tuckerman	"Discussion of Paper by R. L. Templin entitled 'The Determination and Significance of the Proportional Limit in the Testing of Metals,'" Proc. A.S.T.M., Vol. 29, Part II, page 538.
33	1930	Frary, Edwards and Jeffries	"Aluminum Industries." A chemical analysis of the aluminum alloy 3S, and the significance of the cold work symbols ¾H, H and O, may be found on page 232, et. seq.
34	1932	W. Flügge	"Die Stabilität der Kreiszylinderschale," Ingenieur-Archiv., Vol. 3, p. 463.
35	1936	S. Timoshenko	"Theory of Elastic Stability."
36	1925 1926	W. Lode	"Berichte des Werkstoffauschuss," V. D. E. Düsseldorf; also Proc. 2nd Int. Congr. App. Mech., Zurich.
37	1931	A. Nadai	"Plasticity."
38	1940	J. Marin and R. L. Stanley	"Failure of Aluminum Subjected to Combined Stress," Am. Welding Soc. Jour., Vol. 19, Part I, pp. 74s-80s.
39	1939	J. M. Lessells and C. W. MacGregor	"Certain Phases of the Combined Stress Problem," Proc. 5th Int. Congr. App. Mech., Cambridge, Mass.
40	1939	J. L. Holmquist and A. Nadai	"A Theoretical and Experimental Approach to the Problem of Collapse of Deep-Well Casing," Am. Petroleum Inst., Drilling and Production Practice, pp. 392-420.

This page is intentionally blank.

This page is intentionally blank.

This page is intentionally blank.